

Final report for the single sector H2 micromix combustor segment performance and NOx emissions assessment



ENABLE·H2

ENABLING cryogEnic Hydrogen-based CO2-free air transport

Call identifier

H2020-MG-2016-2017/H2020-MG-2017-Two-Stages

Project start

01.09.2018

Project duration

51 months



ENABLEH2

D3.3 -

Final report for the single sector H₂ micromix combustor segment performance and NO_x emissions assessment

Deliverable lead beneficiary: CU

Authors:

Xiaoxiao Sun, Vishal Sethi, Gaurav Singh, Alexandros Giannouloudis, Andrew Rolt, David Abbott, Pierre Gauthier, and Charith Wijesinghe (Cranfield University)

Nicholas Treleaven, Stefano Puggelli, Renaud Mercier, and Julien Leparoux (SAFRAN)

Acknowledgements:

Parash Agarwal, Johannes Berger, Scott Booden, Giulia Babazzi, Francesco Carbonara, Michael Corsar, Alexandros Giannotta, Gary Hann, Kevin Howard, Elzbieta Jarzebowska, Marcos Lopez-Juarez, Jonathan McClure, Devaiah K. Nalianda, Norman Partridge, Celia Anton Pizarro, Alvaro Fogue Robles, Abhay Veer Singh, Malika Zghal

Issue & Date	Internal Auditor	Name, Beneficiary short name	Modifications requested	Date of approval
28-02-2023	WP leader	Xiaoxiao Sun, (Dr)	No	28/02/2023
28-02-2023	Coordinator	Vishal Sethi, (Prof)	No	28/02/2023

Due Date 31.10.2021 (M38)

Actual submission date 28.02.2023 (M51)

Project start date: 01.09.2018

Project duration: 51 months

Dissemination level: Public

Grant Agreement: 769241

Call identifier: H2020-MG-2016-2017/H2020-MG-2017-Two-Stages

Project title: ENABLEH2 – **ENAB**ling cryog**ENic** Hydrogen-based CO₂-free air transport

Contents

1	Abstract	3
2	Glossary	5
3	Introduction	8
3.1	Hydrogen Combustion for Aviation	8
3.2	The Micromix Concept	9
3.3	Overview of the Work Scope of WP3	12
4	Micromix Injector Array Numerical and Experimental Analyses	14
4.1	Numerical Modelling	14
4.1.1	Thermodynamic Modelling	14
4.1.2	Diffusion Modelling for Hydrogen Combustion	15
4.2	Design Space Exploration	18
4.2.1	Design Parameters	18
4.2.2	Numerical Model Setup	19
4.2.3	Key Outcomes	20
4.3	Micromix Injector Array Experimental Rig	22
4.3.1	Rig Overview	22
4.3.2	Injector Manufacturing	23
4.3.3	Test Cases	24
4.3.4	NO _x Results	25
4.4	Altitude Relight Performance Simulations	28
5	H ₂ Micromix Combustor Preliminary Sizing, General Arrangement and Emissions Analyses	30
5.1	Aim of H ₂ Micromix Combustor Preliminary Sizing	30
5.2	Hydrogen Micromix Combustor Architecture	30
5.3	Preliminary Combustor Design and Sizing	31
5.3.1	H ₂ Micromix Combustor Design and Sizing Methodology	31
5.3.2	Assumptions	31
5.3.3	Combustor Component Sizing	33
5.4	H ₂ Micromix Injector Array Design	35
5.5	Implementation	37
5.6	NO _x Emissions Assessment	39
5.6.1	Landing and Take-off (LTO) Cycle	39

5.6.2	Lower Order NO _x Emissions Prediction Model	39
5.6.3	NO _x Emissions Prediction Correlation Development Methodology	40
5.7	Numerical Setup.....	42
5.8	Numerical Simulation Results.....	44
5.8.1	Influence of Pressure	44
5.8.2	Influence of Temperature	45
5.9	NO _x Correlation	46
5.9.1	NO _x Emissions Prediction Correlation Variables.....	46
5.9.2	NO _x Emissions Prediction Correlation	46
5.9.3	H ₂ Micromix EINO _x ISA-SLS Humidity Correction.....	48
5.9.4	Humidity Correction for Altitude	49
6	Thermoacoustic risk assessment and roadmap	50
6.1	Thermoacoustic Risk Assessment.....	50
6.1.1	Introduction.....	50
6.1.2	Thermoacoustic Behaviour of a Hydrogen Micromix Aviation Gas Turbine Combustor Under Typical Flight Conditions	51
6.1.3	Other periodic instabilities	59
6.2	Risk Summary.....	61
6.2.1	Hazards Identification.	61
6.2.2	Risks Assessment	61
6.2.3	Control and mitigation of the risks.	63
6.3	Micromix Combustor Thermoacoustic Design and Development Roadmap	66
7	Conclusions and Recommendation.....	69
	References	72
	Appendix – WP3 Micromix Combustion Publications	76

1 Abstract

For hydrogen(H_2) combustion, a key technical challenge is the research, design, and optimisation of H_2 combustors delivering ultra-low NO_x without any performance, operability, or safety compromises. Jet A-1 has relatively narrow combustion flammability limits which presents several challenges for low NO_x combustion technologies. H_2 has much wider flammability limits enabling leaner (lower flame temperature) combustion. Additionally, the molecular diffusivity and high flame speed of H_2 offer good mixing and lower residence times, therefore significant reductions in NO_x are possible. Micromix (diffusion) combustion enables superior fuel and air mixing without the risks of auto-ignition and flashback that are associated with premixing. The improved mixing reduces local high flame temperature regions, leading to ultra-low NO_x emissions. Within ENABLEH2 WP3, ultra-low NO_x H_2 micromix combustion technology has been matured through a combination of numerical and experimental research comprising injector array and altitude-relight studies. This report presents an overview of this work and the key outcomes.

Best practices for H_2 and air mixing and combustion numerical modelling were established by assessing the influence of different turbulent-chemistry interaction models and species diffusion models on flame characteristics. These CFD best practices were used for H_2 micromix injector design space exploration studies to investigate the impact of key injector design variables on flame characteristics and NO_x emissions. The momentum flux ratio (i.e., jet penetration) was identified as the key parameter that influences the flame interaction, residence time, recirculation zone size, hence NO_x formation. Three injector designs with different flame interaction types were selected for experimental testing.

A dedicated high-pressure, high-temperature hydrogen combustion rig was constructed, with comprehensive health and safety provisions for the high-pressure vessel, safe hydrogen combustion and laser diagnostics. A hybrid approach was adopted for manufacturing the micromix injection system, to ensure minimum hydrogen leakage, as well as good sub-millimetre hole quality. The three micromix injector arrays (~30 injectors each) were tested at various operating conditions (combustor inlet temperature up to 585K and pressure up to 10 bar_a, and equivalence ratio from 0.3 to 0.5).

Both numerical and experimental results suggest that a relatively low momentum flux ratio injector design has the potential to achieve the lowest NO_x , and that NO_x increases significantly for equivalence ratios above 0.4. The measured NO_x was more than 50% lower than a state-of-the-art Jet A-1 combustor at similar conditions.

Altitude relight numerical simulations were performed for various combustor inlet and equivalence ratio conditions. For the low momentum flux ratio, low NO_x design, a single spark may be sufficient for ignition at relatively lower altitudes. However, for high altitude, multiple sparks may be needed. Altitude ignition performance could be improved by increasing the equivalence ratio to stoichiometric, which results in increased jet penetration, higher flame speed and larger recirculation zones thereby improving ignitability with a single spark.

A dedicated thermoacoustic instability risk assessment was performed. This included identifying potential instabilities, their frequencies and mitigation strategies. A micromix combustor is less likely to produce low frequency (<1000Hz) instabilities and any high frequency instabilities can be mitigated by modifying flame or system acoustics, for example by fuel staging and/or implementing Helmholtz resonators.

The research also included the preliminary sizing, general arrangement, and NO_x emissions analyses of a H₂ micromix combustor for a high bypass ratio turbofan engine for a Year 2050 LR BWB aircraft. It is expected that a low NO_x micromix combustor of such an engine will require ~11000 injectors with an energy density of 6.7MW/(bar-m²). A lower-order NO_x emissions prediction correlation was derived from higher fidelity CFD simulations. The correlation predicts the value of NO_x emissions as function of combustor inlet temperature and pressure, equivalence ratio and ambient humidity. The correlation was used for aircraft mission-level assessments, and it is estimated that, relative to the Year-2050 long-range Jet A-1 tube & wing design, NO_x is reduced by 39-43% for the LH₂ tube & wing aircraft and by 54-59% for the more efficient LH₂ BWB aircraft.

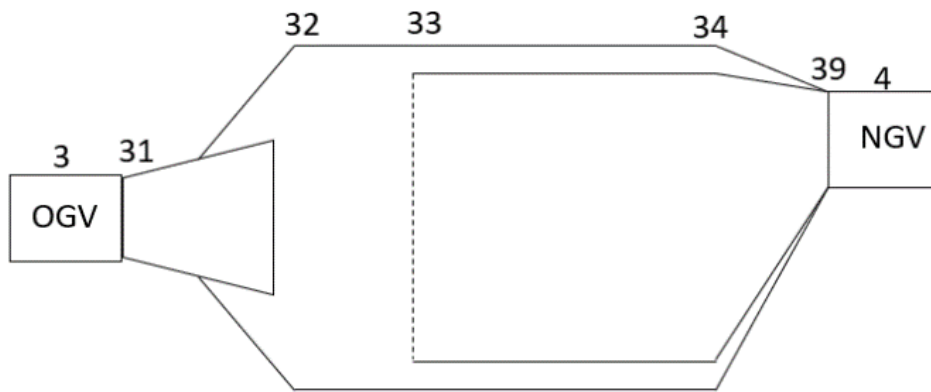
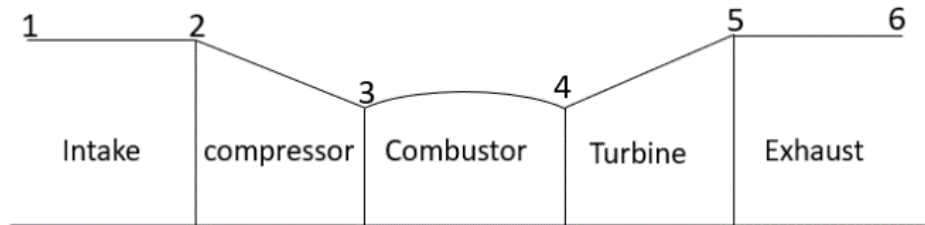
The report concludes with several recommendations to expedite entry into service of low-NO_x hydrogen micromix combustion systems.

2 Glossary

Abbreviation	Description
ACARE	Advisory Council for Aviation Research and Innovation in Europe
Bar _a	Absolute pressure in bar
CA	Consortium Agreement
CC	Complex Chemistry
CFD	Computational Fluid Dynamics
CO ₂	Carbon Dioxide
DEL	Deliverable
DoA	Description of Action
DOE	Design of Experiments
D _p	Measured Mass of Emissions in grams
EDC	Eddy Dissipation Concept
EEINO _x	Energy-based Emissions Index of NO _x (g/MJ)
EI	Emission Index
EINO _x	Emission Index of Nitric Oxides (g/kg)
FAR	Fuel to Air Ratio
FGM	Flamelet Generated Manifold
F ₀₀	Rated Static Thrust of Engine (kN)
FTF	Flame Transfer Functions
GEO	Combustor Geometry
H ₂	Hydrogen
H ₂ O	Water
ICAO	International Civil Aviation Organization
IRZ	Inner Recirculation Zone
JICF	Jets-In-Crossflow
LDI	Lean Direct Injection
LES	Large Eddy Simulation

LFC	Laminar Flame Concept
LHS	Latin Hypercube Sampling
LHV	Lower Heating Value
LTO	Landing and Take Off Cycle
MFC	Mass Flow Controller
MLDI	Multipoint Lean Direct Injection
N ₂	Nitrogen
NO _x	Oxides of Nitrogen
O ₂	Oxygen
ORZ	Outer Recirculation Zone
P	Pressure (kPa)
PB	Pebble Bed
PHI	Equivalence Ratio ($FAR_{actual} / FAR_{stoichiometry}$)
RANS	Reynolds-Averaged Navier-Stokes
RO	Rated Output Thrust (kN)
SST	Shear Stress Transport
T	Temperature (K)
TERA	Techno-Economic Environmental Risk Assessment
TIM	Time-In-Mode (s)
TRL	Technology Readiness Level
WP	Work Package
m_f	Fuel Flow Rate (kg/s)
ΔP_{fa}	Differential pressure of fuel and air
ΔP_C	Combustor fractional pressure loss
ΔP_{AG}	Air gate fractional pressure loss
T_{ad}	Combustor adiabatic flame temperature (K)
ϕ	Equivalence Ratio
ω	Specific Humidity (kg/kg)

Station Number Subscripting Adopted



3 Introduction

3.1 Hydrogen Combustion for Aviation

Flightpath 2050 targets very ambitious reductions in CO₂ (75%) and NO_x emissions (90%) relative to Year 2000 technologies. It will be very challenging to meet these targets with conventional fuels with more efficient aircraft and propulsion systems, even when coupled with improved asset management. Even if we were able to meet these targets, this would not be sufficient for a fully sustainable future for civil aviation particularly considering the rate at which other sectors are decarbonising. Greening civil aviation is key to our global future, and it is imperative to succeed without the vast economic and social damage that would follow constraining aircraft demand and operations. So radical aircraft propulsion technologies must be developed urgently. Most likely to succeed in this grand challenge (promising full decarbonisation) are hydrogen (H₂) and electrification. H₂ is an inevitable solution for a fully sustainable aviation future, via hybrid/electric/fuel cell technologies for short to medium range and H₂ combustion in gas turbines for longer missions. However, the huge financial investments required to make this a reality will not be considered until several technical challenges can be overcome. The EU FP5 Cryoplane project [1] (led by Airbus) in the early 2000s was a flagship project for H₂. It concluded that there were no technical showstoppers, but at the time the costs associated with its introduction damped enthusiasm. Nevertheless, there is an increasing consensus that these costs are justified considering the important environmental and socio-economic benefits of sustainable aviation.

H₂ combustion will eliminate mission-level CO₂, CO, unburnt hydrocarbons and particulates, except for minimal contributions due to oil consumption. Since H₂ has much wider stability limits than Jet A-1 or methane, despite higher flame temperature at stoichiometric conditions, it is possible to employ leaner combustion with hydrogen in order to achieve ultra-low thermal NO_x production. Furthermore, the molecular diffusivity and high flame speed of hydrogen facilitates quicker mixing and lower residence time, reducing not only NO_x production but also the combustor length.

H₂ combustion will however generate significantly more water vapour emissions which will increase the likelihood of contrails. However contrails may be completely eliminated by appropriate aircraft mission management. Contrails, contrail avoidance measures and their implications for H₂-fuelled aircraft are elaborated in ENABLEH2 public deliverable D1.4 [2].

The exceptionally high heat capacity of H₂ also provides a formidable heat sink, which can be used to produce engine concepts with much higher engine thermal efficiency and can facilitate the application of superconductivity in more advanced propulsion systems.

3.2 The Micromix Concept

Hydrogen micromix combustion utilises an array incorporating a large number of H₂ flames at very lean conditions to enhance mixing and limit flame temperature, hence the production of NO_x. The concept is based on the Jet-In-Crossflow (JICF) principle, where a jet of fuel penetrates a crossflow of air at a 90° angle, as shown in Figure 3-1. H₂ is injected via a small orifice into accelerated air exiting the air gate. The small injectors and high fuel velocity ensure that the flames are miniaturised but highly intensified. The small spatial scale, along with very good mixing properties of the JICF allow more homogeneous fuel-air mixtures to form. Improved local mixing leads to lower flame temperatures and lower NO_x emissions. As there is no fuel-air pre-mixing upstream of the combustion chamber, the risks of flashback and auto-ignition are inherently low.

Various geometrical parameters influence the design and emissions of a micromix combustion system. They are defined in Figure 3-1 and include the air gate width, air gate height, the aspect ratio, H₂ injection orifice diameter, air/ H₂ offset distance (i.e. the length between the air gate and H₂ injection) and the mixing distance from H₂ injection to the trailing edge of the injector plate. The vertical and horizontal spacing of the injectors are also design parameters.

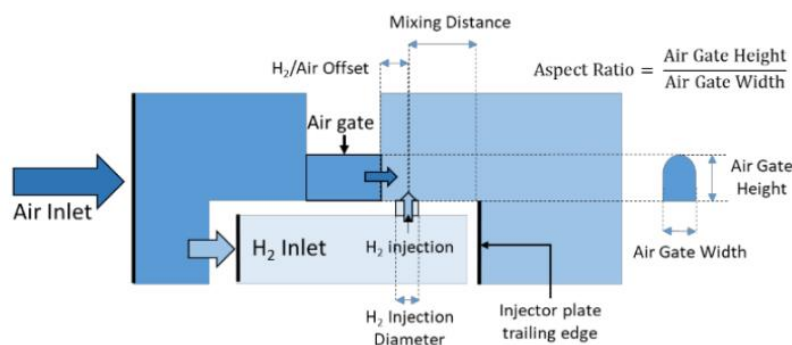


Figure 3-1: H₂ micromix single injector geometric features [3]

In order to design micromix injectors for low NO_x emissions, it is critical to identify the position of H₂ jet penetration, which has a dominant role on characteristics of the flame. The ideal flame position is in the shear layer that forms between the two interacting streams and the two recirculation zones (inner and outer vortices – Figure 3-2) that form around the streams. This position avoids the flames being entrained in either of the recirculation zones, which could lead to merged flames and hence higher temperatures, as well as increased residence time, both of which lead to higher NO_x.

For a JICF, the Momentum Flux Ratio (MFR) between the fuel jet and the air crossflow is the key parameter that determines the penetration of the hydrogen jet.

The momentum flux ratio is defined as:

$$J = \frac{\rho_j v_j^2}{\rho_{CF} v_{CF}^2} \quad \text{Equation 1}$$

Where ρ_j represents the density of H₂, ρ_{CF} represents the density of the free stream air and the v_j represents the H₂ flow velocity, v_{CF} represents the velocity of the air at air gate exit.

The higher the momentum flux ratio, the greater the penetration of the H₂ stream into the air stream.

The optimum MFR is when the H₂ has sufficient penetration in the air, this ensures sufficient fuel-air mixing, and the flame is positioned predominantly within the shear layer between the vortices formed by outer and inner recirculation shown in Figure 3-2. Under penetration will result in flame trapped in the inner recirculation zone shown in Figure 3-3(a) while over penetration will result in flame merging downstream of the outer recirculation as depicted in Figure 3-3(b) both of which are undesired.

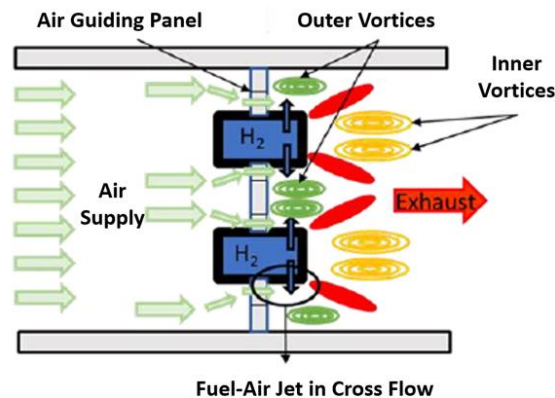


Figure 3-2: Fuel-air interaction in JIC with ideal flame placement in shear layer

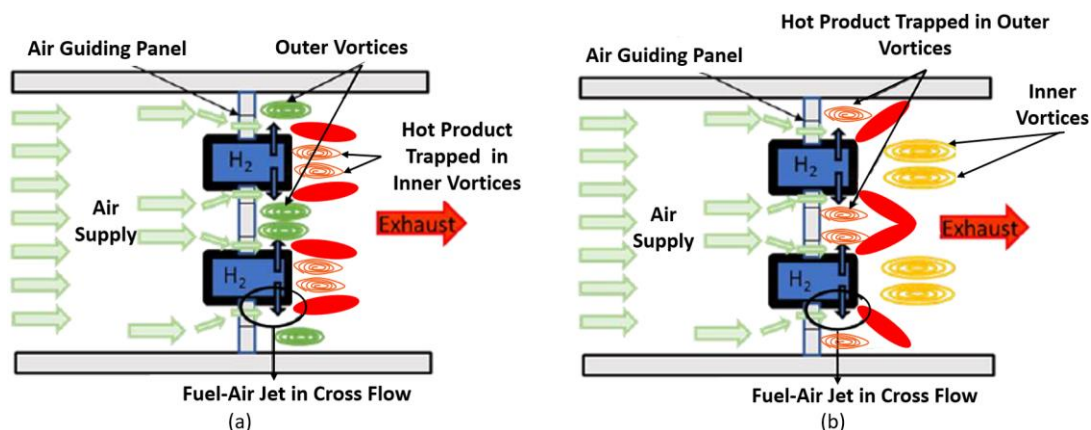


Figure 3-3: Undesired interaction of flames (a) from the same fuel feed arm (relatively lower MFR), (b) undesired flame interaction from neighbouring injectors (relatively higher MFR).

As shown in Figure 3-4, unlike conventional Jet A-1 combustors, the H₂ micromix combustor concept uses many small injectors, resulting in many small hydrogen flames burning at very lean conditions. This configuration offers the ability to stage the fuel distribution circumferentially and radially, resulting in the added capability to control the following:

- The outlet temperature distribution (pattern factor) without the use of dilution holes. This is important to maximise turbine blade creep life.
- The thermoacoustic behaviour of the combustor to mitigate undesired instabilities.
- NO_x emissions control and reduction over the whole aircraft mission

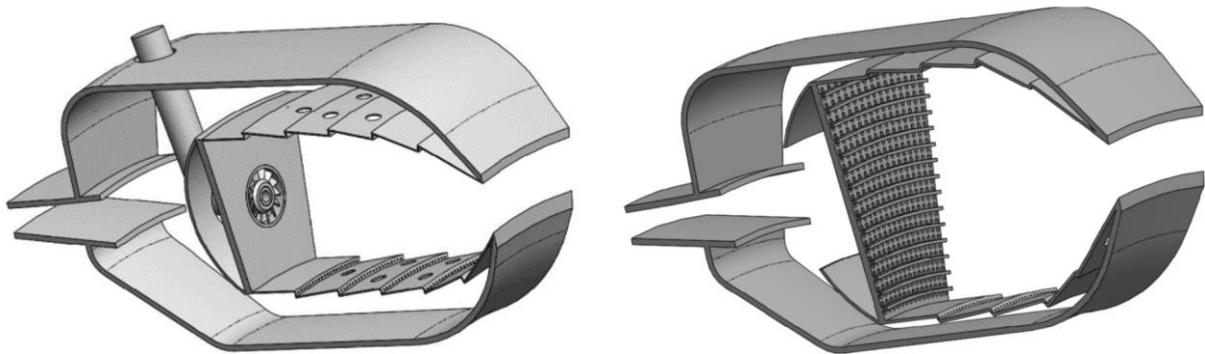


Figure 3-4: CAD illustration of a section of a conventional (left) and a hydrogen micromix (right) combustor

3.3 Overview of the Work Scope of WP3

The following research and innovation activities on H₂ micromix combustion were conducted in WP3:

- Numerical modelling of hydrogen micromix combustion, including developing best-practices for hydrogen combustion modelling using state-of-the-art commercial CFD software.
- Injector design space exploration to investigate the effect of various design parameters on flames, their interactions, and emissions characteristics. This allowed down selection of potential low-NO_x designs for experimental testing.
- Development of an instrumented high-pressure high-temperature hydrogen lab-scale combustion rig for proof of concept and data acquisition (pressure loss, exit temperature, NO_x and thermoacoustic instabilities).
- Experimental testing on down-selected injectors to obtain performance and emissions characteristics for micromix flames to identify designs which have the potential to achieve ultra-low NO_x. Comparison of emissions data between numerical and experimental results, analysis of NO_x emissions trends with variations in operating conditions.
- High-fidelity numerical simulations of altitude relight conditions including the effects of altitude and fuel equivalence ratio on relight performance.
- Preliminary aerodynamic sizing and general arrangement of a hydrogen micromix combustor for a high bypass ratio turbofan engine for a Year 2050 long range, blended wing body aircraft (LR BWB 2050). Assessment of combustion performance and operability characteristics.
- Development of a lower order NO_x emissions prediction correlation for a hydrogen micromix combustor based on numerical simulations capturing the effect of boundary conditions (namely equivalence ratio, combustor inlet temperature and pressure, and ambient humidity).
- Thermoacoustic risk assessment of hydrogen micromix combustor for aero engines at typical flight conditions. Identification of potential combustion instability mechanism and mitigation methods.
- Dedicated hydrogen micromix combustor thermoacoustic risk assessments and roadmap. (Section 6)

This report provides detailed information on:

- The hydrogen micromix combustion concept and key injector design variables (Section 3)
- Micromix injector array numerical and experimental analyses (Section 4)
 - H₂-air mixing and combustion numerical modelling with design space exploration and thermoacoustic instability analyses
 - Development of a high-pressure high-temperature H₂ combustion rig, health and safety provisions, and combustion testing outcomes for three micromix injectors at various operating conditions (combustor inlet temperature and pressure, and equivalence ratio)
 - Altitude relight numerical simulations at various combustor inlet and equivalence ratio conditions.

- The preliminary sizing, general arrangement, and NO_x emissions analyses of a H₂ micromix combustor for a high bypass ratio turbofan engine for a Year 2050 aircraft (Section 5)
- A summary of the lessons learnt, new research gaps identified and recommendations for further work (Section 7)

4 Micromix Injector Array Numerical and Experimental Analyses

4.1 Numerical Modelling

Computational Fluid Dynamics (CFD) is widely used for design space exploration as well as emissions prediction for novel combustion technology development. In order to minimise time and costs, simplified combustion CFD models have been developed to account for the effect of turbulence on reactions, coupled with Reynolds-Averaged Navier-Stokes (RANS) or Large Eddy Simulation (LES) turbulence models. These models often employ assumptions and model constants that have been specifically calibrated for conventional fuels such as Jet A-1 and natural gas to match experimentally derived flame and emissions characteristics. Due to its very low molecular weight, H₂ has significantly different characteristics relative to other hydrocarbon fuels and other species within the mixture. These specific properties of H₂ invalidate a number of assumptions that are made when modelling mixing and combustion using simplified models and model constants. For H₂-air mixtures, there is a need to further investigate and understand the impact of such modelling assumptions. Additionally, the turbulent characteristics in a jets-in-crossflow mixing process have a further impact on the overall hydrogen diffusion rate. Conventionally, it is believed that for high Reynolds Number cases, turbulent diffusion is dominant and that differential and preferential diffusion only have a minor effect.

There is limited numerical and experimental data on flame characteristics and emissions of hydrogen micromix combustors at high pressure and temperature conditions. Appropriate modelling of these effects is essential for reaction rate, flame temperature and emissions predictions.

4.1.1 Thermodynamic Modelling

Thermodynamic modelling was used to calculate the transport coefficients and non-dimensional parameters, for all species in the H₂-air reaction mechanism.

The transport characteristics of the mixture are often characterised by the Schmidt (Sc), Lewis (Le) and Prandtl (Pr) numbers:

$$Sc = \frac{\nu}{D} = \frac{\mu/\rho}{D} \quad \text{Equation 2}$$

$$Le = \frac{\alpha}{D} = \frac{k/\rho C_p}{D} \quad \text{Equation 3}$$

$$Pr = \frac{\nu}{\alpha} = \frac{Sc}{Le} \quad \text{Equation 4}$$

The dynamic viscosity μ , thermal conductivity k and specific heat capacity C_p are solely functions of temperature and were obtained from published NASA polynomials [4].

Modelling the diffusion coefficient can be simplified as a Fickian process. The mixture averaged diffusion coefficient D'_{km} for species k into mixture m is a function of temperature and mixture composition and was calculated for each species using:

$$D'_{km} = \frac{1 - Y_k}{\sum_{j \neq k}^N \frac{X_j}{\mathcal{D}_{kj}}} \quad \text{Equation 5}$$

Where Y_k is the mass fraction of species k , X_j is the mole fraction of species j , \mathcal{D}_{kj} is the binary diffusion coefficient of species k and j .

With the non-dimensional parameters calculated, the impact of boundary conditions, such as inlet pressure, temperature, equivalence ratio on the transport characteristics could be better understood. For example, for air inlet conditions i.e. $200\text{K} \leq T_{in} \leq 1000\text{K}$, $1\text{bar} \leq p_{in} \leq 20\text{bar}$, the effect of pressure can be neglected. The effect of temperature is significantly smaller than the effect of equivalence ratio. At $\phi \sim 0.4$ (lean combustion), $Sc \sim 0.22$, $Pr \sim 0.75$ and $Le \sim 0.3$ for the mixture. These values are far from unity, which is often assumed for combustion with hydrocarbon fuels.

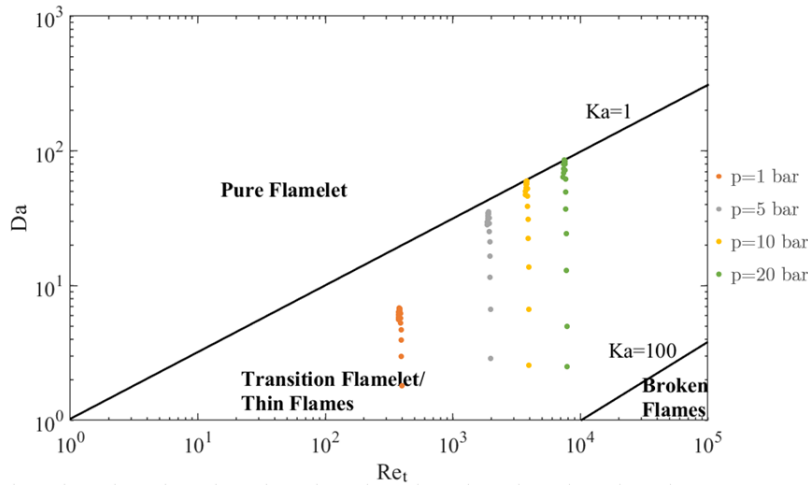


Figure 4-1: Characterising H_2 micromix flame regime. Operating conditions: $p \in (1,5,10,20)$ bar and $\phi \in [0.5,2]$ (diffusion flame) for $T_{in} = 600\text{K}$ and $T_{H_2} = 300\text{K}$

The flame regimes can then be determined based on the Damköhler (Da), Karlovitz (Ka) and turbulent Reynolds (Re_t) numbers, with appropriate assumptions for the turbulent characteristics of the flow. An example of the flame regime diagram for non-premixed flames is shown in Figure 4-1 with micromix flames plotted at several pressure and equivalence ratio conditions. These flames are characterised as transition flamelets, which can be modelled using flamelet based models or thickened flame models.

4.1.2 Diffusion Modelling for Hydrogen Combustion

Within STAR-CCM+, when complex or detailed chemistry models are enabled, transport equations (e.g., Equation 6) are solved for each species.

$$\frac{\partial}{\partial t} \rho Y_i + \frac{\partial}{\partial x_j} (\rho u_j Y_i + F_{k,j}) = \dot{\omega}_i \quad \text{Equation 6}$$

Where Y_i is the species mass fraction, $F_{k,j}$ is the diffusion flux, and $\dot{\omega}_i$ is the source term. The diffusion flux term $F_{k,j}$ can either be modelled by the Fick's law, or by the multi-component diffusion model based on kinetic theory.

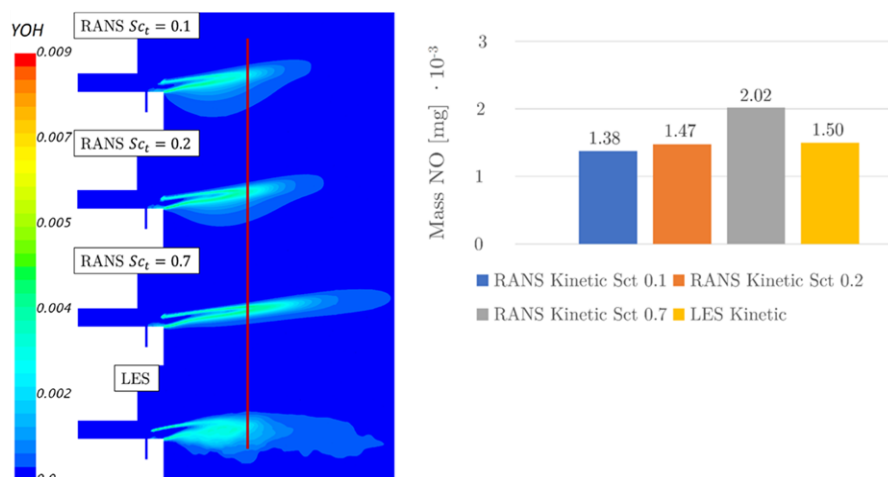


Figure 4-2: Effect of S_{ct} and comparison with LES (Left: contours of the mass fraction of OH; right: mass of NO_x in the flame region)

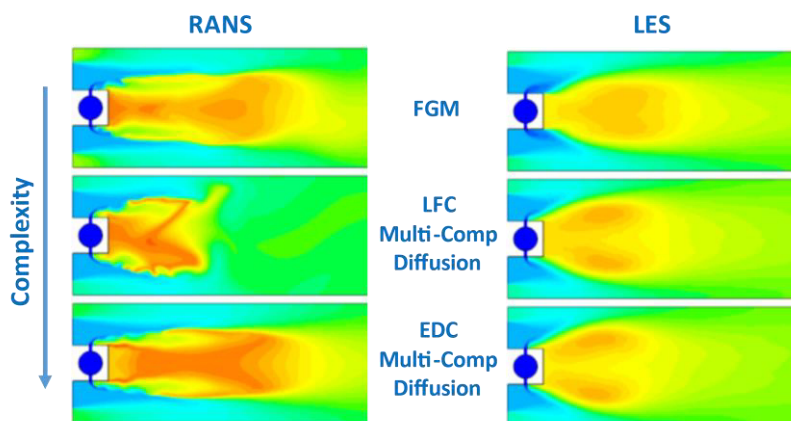


Figure 4-3: RANS vs. LES, tabulated chemistry (FGM) vs. Complex chemistry with multi-component diffusion

Sensitivity studies were conducted with complex chemistry Laminar Flame Concept (LFC) in STAR-CCM+ using three different diffusion coefficients models (mixture averaged, multi-component with and without thermal diffusion). All the simulations yielded flame lengths and temperatures of a similar order. The inclusion of the thermal diffusion does not significantly vary the flame temperature; however, it does have a noticeable impact on flame structure and stability. The effect of turbulent transport numbers, such as turbulent Schmidt number, have a more significant impact on the flame length and temperature. The turbulent Schmidt number was calibrated to 0.2 based on the JICF structure and comparison to LES results (Figure 4-2).

Figure 4-3 summarises a comparison between RANS and LES with different diffusion modelling fidelities. LES yielded flames of similar length for complex chemistry (both LFC and Eddy Dissipation Concept (EDC)) and Flamelet Generated Manifold (FGM), with a lower time-averaged temperature than their respective RANS flames. For the LES, the flame structures were not affected by the choice of EDC or LFC when using CC. This is not the case when using RANS where the flame structures predicted when using either LFC or EDC differ significantly. Both complex chemistry models i.e., EDC and LFC, form two discrete hot cores

whereas FGM forms a single hot core, owing to thermo-diffusive effects (preferential diffusion or thermal diffusion) captured by the complex chemistry. Meanwhile, the similarity in flame length and insensitivity to closure type demonstrates the dominance of turbulent effect in determining flame structure, through turbulent mixing.

Hence for H₂ micromix combustion modelling, LES should be adopted wherever affordable. RANS are generally overly sensitive to the turbulence-chemistry interaction, which are governed by both the models and constants used. Flame length and temperature could vary significantly. With LES, this uncertainty is significantly reduced. Multi-component diffusion with a complex chemistry model should be used with LES to capture the impact of differential diffusion, which more accurately predicts a (higher) flame temperature than simpler chemistry models (that are less computationally expensive).

4.2 Design Space Exploration

4.2.1 Design Parameters

The key geometric design features of the micromix injector which impact the aerodynamic mixing of the two flows (H₂ fuel and crossflow air) are shown in Figure 4-4. Evaluating the impact of these design features and their impact on performance and emissions is essential to design a lean burn ultra-low NO_x micromix combustion system. An extensive numerical and experimental investigation has been conducted at Cranfield University to develop an ultra-low NO_x injector design as reported in Refs[3], [5].

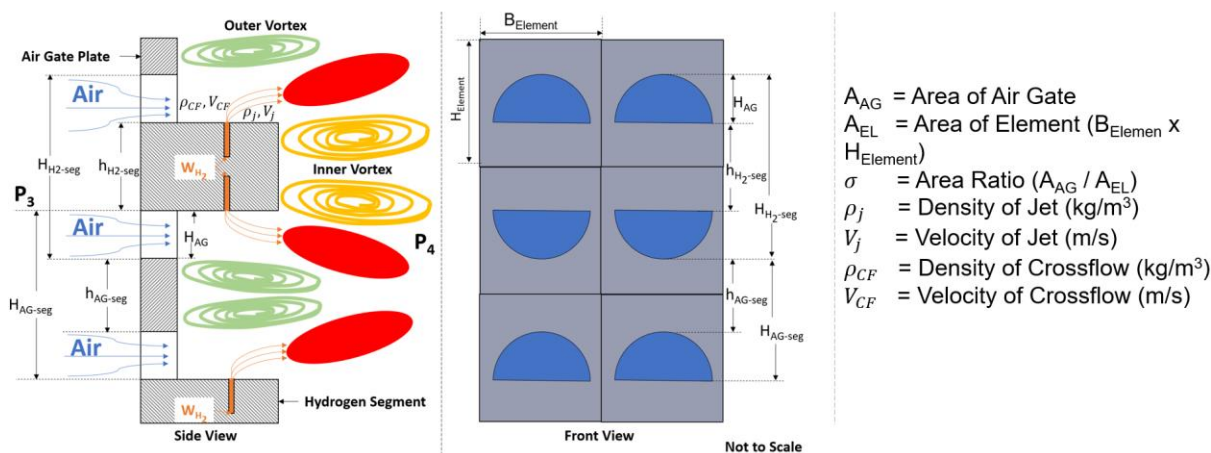


Figure 4-4: Micromix injector geometric variables

A design space exploration study was conducted by varying the design parameters of the micromix injector. The H₂ orifice diameter, the air gate dimensions, and the H₂/air offset distance and mixing distance were varied as a part of this analysis. The range of the design variables investigated in the study are presented in Table 4-1.

Table 4-1 – Injector design parameters variation ranges for design space exploration

Design Parameter	Range
H ₂ Offset Distance	0.5 – 5 mm
Mixing Distance	0.5 – 5 mm
Vertical Injector Distance	5 mm
Horizontal Injector Distance	5 mm
H ₂ Inlet Diameter	0.3 mm
Air Gate Aspect Ratio	1- 2
Air Gate Height	1 – 2.5 mm
Air Gate Diameter	1 – 2.5 mm

Several selection criteria were used to down select the injector designs for rig testing. The injector designs needed to cover a range of momentum flux ratios, offset distances and mixing

distances to ensure that different flame lengths, positions and shapes could be observed. This also ensured that various types of flame interactions could be observed, such as: no interaction, interaction within the inner recirculation zone between flames sharing same feeding arm and interaction between flames of jets from neighbouring feeding arms downstream of outer recirculation zone.

4.2.2 Numerical Model Setup

The numerical domain is illustrated in Figure 4-5. It consists of a single “arm” comprising two micromix injectors including two air gates and two hydrogen injection orifices. Both the hydrogen and air inlets were considered as mass flow inlets. To represent a very large injector array, periodic boundaries were imposed. The exit of the domain is at 60mm downstream of the hydrogen injection and set to pressure outlet. For all cases in this study the operating pressure was set to 15 bar, the hydrogen and air inlet temperatures were set to 300K and 600K respectively and an equivalence ratio of 0.4 was selected.

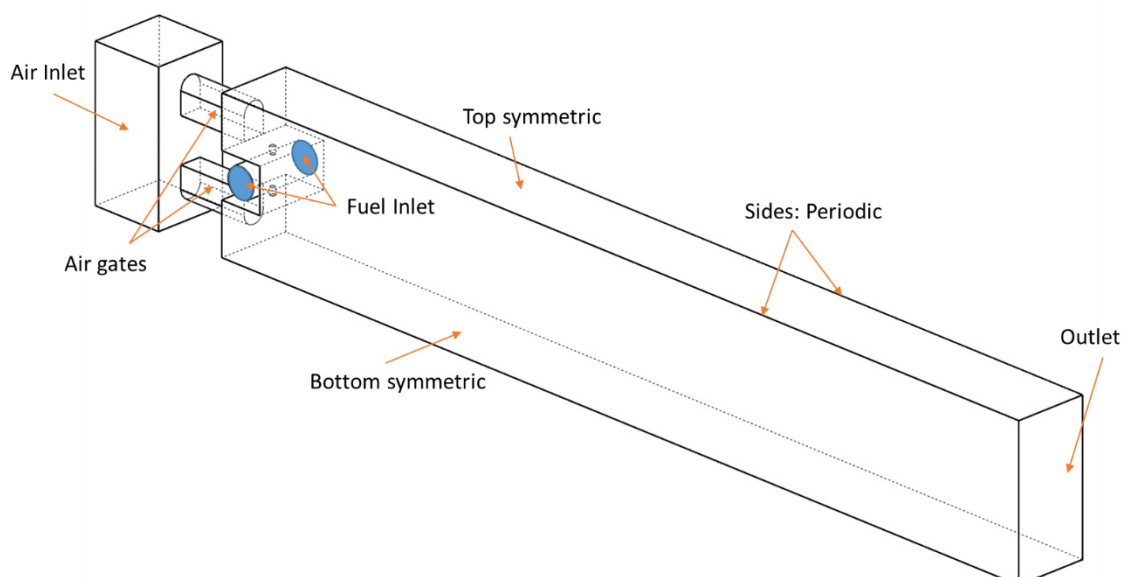


Figure 4-5: Numerical domain for injector design space exploration study

The mesh size was determined via a grid independence study, to ensure that the computational cost would be acceptable without compromising the accuracy. The flame region was refined with a cell size of 0.08mm with 10 prism layers in the vicinity of the wall.; a $y^+ < 2$ was used for walls within the flame region. Downstream of the estimated recirculation area, the mesh size was kept close to 0.3mm.

The k-omega SST turbulence model was used as the shear stress transport (SST) formulation allowing for integration down to the wall through the viscous sub layer, resulting in a more accurate near wall treatment [6]. This is vital for designs involving JICF, ranging from miniaturised mixing characteristics close to the hydrogen jet to the larger eddies in the combustion zones with presence of shear layers and strong recirculation. The fluid was considered as a compressible ideal gas. The FGM combustion model was used with the model constant settings outlined in Section 4.1.

4.2.3 Key Outcomes

The temperature of the flame and post-flame zones, in conjunction with residence time are the most important factors that affect the production of thermal NO_x. Fuel lean combustion results in lower flame temperatures (relative to Stoichiometric), hence lower NO_x.

In predominantly diffusion flames, such as micromix, although a global (lean) equivalence ratio may be assumed based on a total fuel to air flow ratio, the fuel and air mixture is not homogenous. This will result in local fuel rich pockets and regions of stoichiometric mixtures that produce high local flame temperatures regions and more NO_x. Thus, mixing of the hydrogen and air, as well as of the unburnt and burnt gas (flame interactions), are dominating factors that influences flame and product temperatures and subsequently NO_x formation.

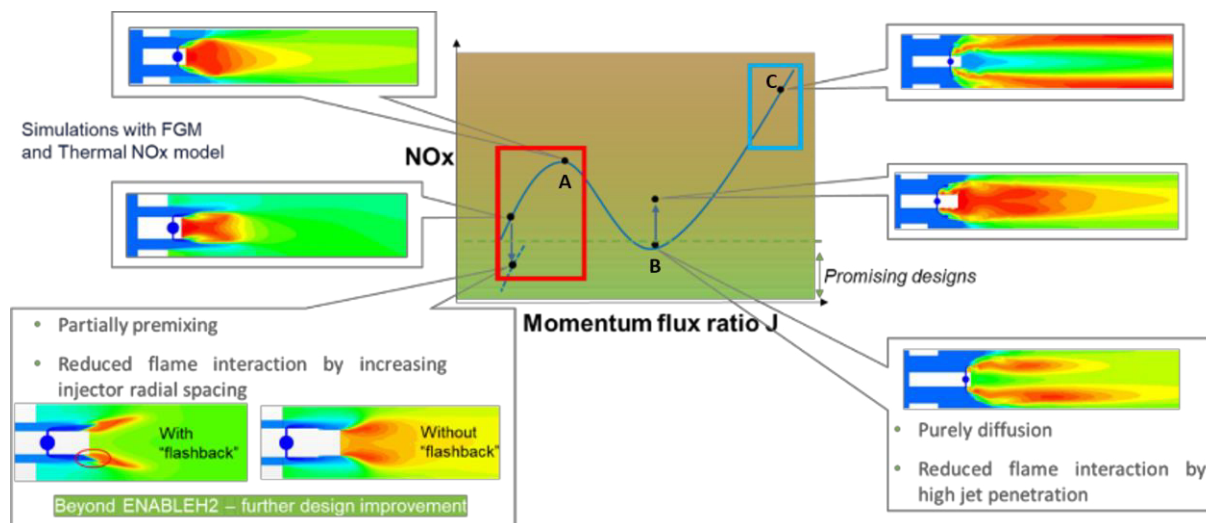


Figure 4-6: Influence of momentum flux ratio on flame characteristics, flame separation, flame interactions and NO_x emissions.

Figure 4-6 shows, in a qualitative way, the expected NO_x emissions levels and different flame patterns for different momentum flux ratio values. The low and medium MFR designs are in the region of the red rectangle. The low MFR configuration was expected to produce flames stabilised in the inner recirculation zone and close to the metal wall of the injectors, while the medium momentum flux ratio design was expected to generate flames that were stabilised in the same region, but further away from the wall. These hypotheses were confirmed by the numerical simulations. The high MFR designs, are in the region of the blue rectangle. Due to the high jet penetration, there is more interaction between the flames of neighbouring injectors, which results in long flames merging downstream of the outer recirculation zones. This results in higher residence time and therefore higher NO_x.

The main geometric parameters of the three injector configurations down selected for the experimental campaign are provided in Table 4-2. They represent a broad range of momentum flux ratios.

Table 4-2 - Main geometric parameters for the three injector configurations

Design	Typical MFR value¹	D (Air) (mm)	Air Gate Height (mm)	Aspect Ratio
Low MFR	0.64	2.10	1.05	0.50
Medium MFR	2.06	1.50	2.25	1.50
High MFR	6.34	2.16	2.85	1.33

¹ Values taken for conditions at 10bar_a pressure, 600K air-inlet temperature and $\Phi=0.4$. Calculation based on fuel temperature of 300K

4.3 Micromix Injector Array Experimental Rig

4.3.1 Rig Overview

A high-pressure, high air-inlet temperature experimental rig was designed for the hydrogen micromix combustion experiments to test micromix injector geometries with different momentum flux ratios, over a range of conditions (namely, inlet pressure, air-inlet temperature, and equivalence ratio). With the instrumentation set up, data for NO_x emissions, dynamic pressure and flame imaging could be obtained.

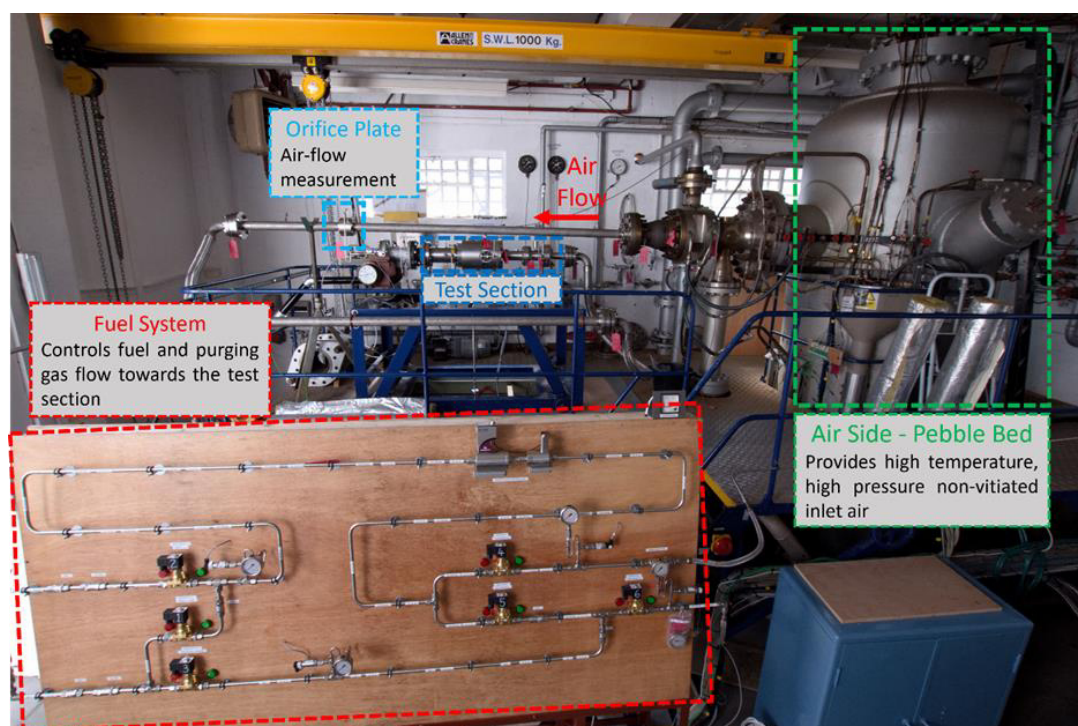


Figure 4-7: Layout of the air-supply system, test section and fuel system

To ensure safety, several operational and design measures were taken. Hydrogen gas detectors as well as ventilation devices were installed in the test house. The test house doors were always kept open and in conjunction with the fans would prevent accumulation of flammable concentrations of hydrogen in case of a leak. To minimise potential sources of hydrogen leakage, the micromix burner was designed as a one-piece component with an isolated chamber for the fuel to be supplied to the injectors. As a further safety measure, the combustion chamber wall thickness was set to 100mm, allowing it to contain a small-scale detonation. The fuel delivery system was customised with five different operational modes for safe ignition, combustion and purging of hydrogen.

The combustion air was supplied by facility compressors and heated by the Pebble Bed (PB) air heater (Figure 4-7). The Pebble Bed is a regenerative heat exchanger that can provide non-vitiated clean air at high temperature and high pressure, reaching temperatures up to 1800K, pressures up to 15bar_a and mass flow rates up to 4kg/s, which are often conditions representative of the combustor inlet of a typical industrial gas turbine, or close to cruise for an aero engine combustor.

A CAD representation of the test rig cross-section with descriptions of its main characteristics and capabilities is shown in Figure 4-8. Optical access provisions allowed for flame imaging techniques to be applied, while thermoacoustic instabilities were measured by employing four dynamic pressure sensors with a loudspeaker creating the acoustic forcing signal. A single-point probe was used to draw the hot gas sample and supply it to the gas analyser (Horiba PG-250) for NO_x emissions measurements. The setup also consisted of a heated sample line to prevent water vapour condensation, a vacuum pump, a membrane dryer stage and a further drying stage that consisted of a drain separator and chiller unit.

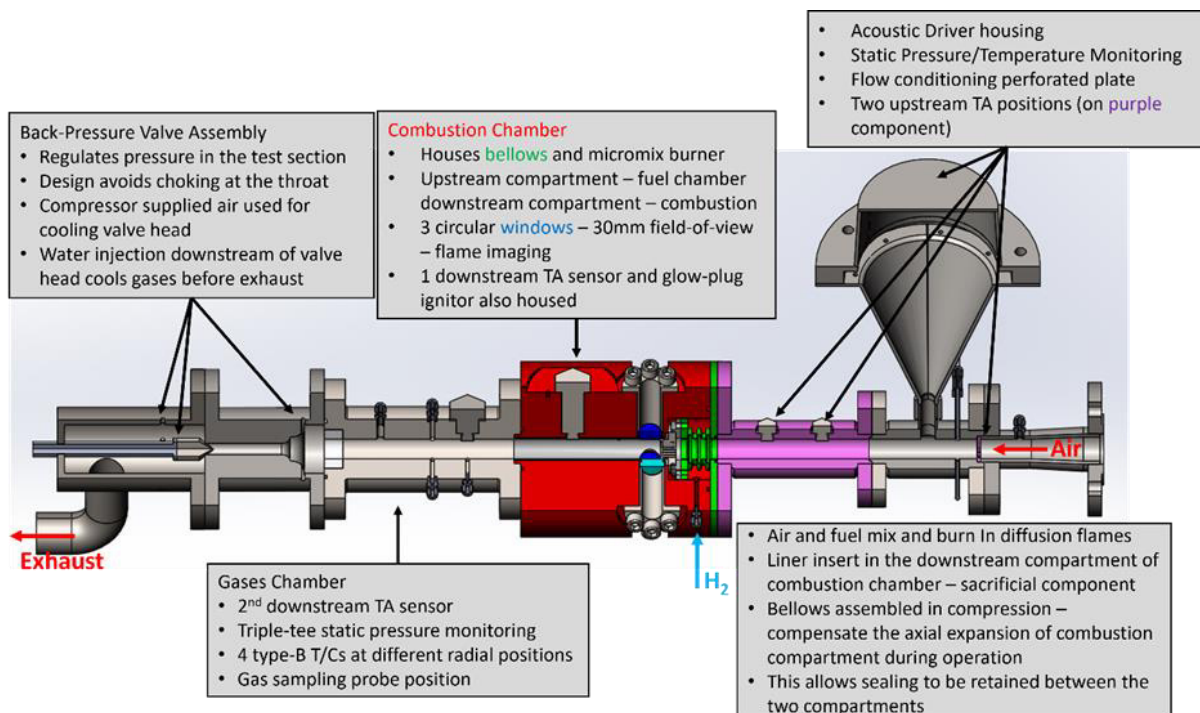


Figure 4-8: CAD representation of the test rig cross-section with descriptions of key components.

4.3.2 Injector Manufacturing

A hybrid manufacturing approach was adopted for the micromix burner. Metal additive manufacturing (AM) and material removal techniques were combined to produce a one-piece component (Figure 4-9). Such a design allows the creation of internal channels on the body of the burner, ensuring safe fuel delivery to the injectors.

Sub-millimetre features, such as the 0.3mm hydrogen injection holes, produced by two AM techniques, namely Direct Metal Laser Sintering (DMLS) and Binder-Jetting Technology (BJT) were not able to achieve acceptable quality. Hence, these holes were drilled by micro-Electrical Discharge Machining (micro-EDM). A tolerance on nominal diameter of $\pm 10\mu\text{m}$ could be achieved. However, this increased the manufacturing cost and time significantly.

Apart from the difficulties in producing micro injection holes, there were other challenges encountered, including internal passage collapsing, as well as de-powdering which required design modifications e.g., longer air gates. There is a need of more advanced manufacturing techniques to facilitate hydrogen micromix burner fabrication.

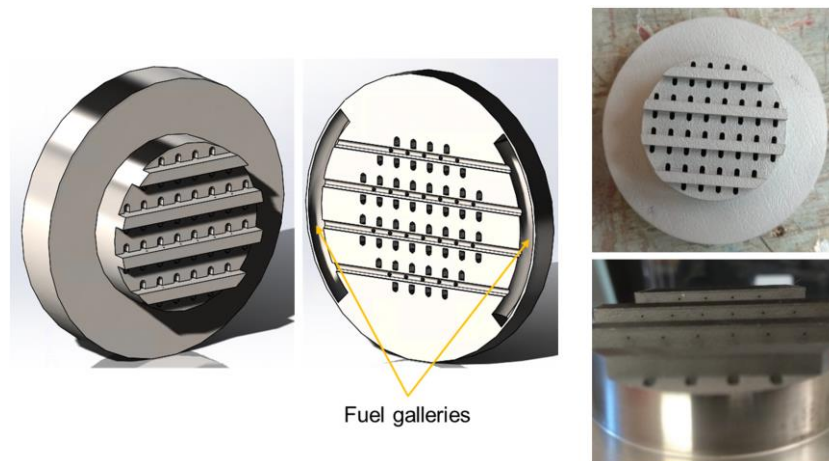


Figure 4-9: Micromix injector array showcasing the air gates, fuel galleries and fuel injection holes

4.3.3 Test Cases

The three different injector configurations (presented in Table 4-2) that were down selected based on the numerical design space exploration study were tested. The test cases are summarised in Table 4-3. The values targeted for inlet pressure were 5bar_a and 10bar_a, for air-inlet temperature were 450K and 600K, and for equivalence ratio were 0.3, 0.4 and 0.5.

Table 4-3: Test Cases for all 3 injector designs (Pressure in bar_a, Temperature in K)

Low MFR				Medium MFR				High MFR			
P _{in}	T _{in}	Φ	ΔP/P	P _{in}	T _{in}	Φ	ΔP/P	P _{in}	T _{in}	Φ	ΔP/P
5.07	316	0.297	9.8%	4.90	447	0.304	3.7%	5.16	422	0.300	1.0%
5.02	315	0.401	9.9%	4.90	446	0.403	3.9%	4.91	421	0.387	1.0%
5.02	314	0.490	10.4%	4.90	446	0.514	4.5%	4.96	422	0.526	1.0%
4.92	590	0.308	7.5%	4.78	574	0.304	4.0%	4.99	582	0.303	1.2%
5.12	585	0.398	7.7%	5.04	579	0.385	3.8%	5.10	577	0.408	1.2%
5.00	595	0.506	8.1%	5.12	584	0.496	3.8%	5.06	581	0.517	1.2%
9.99	457	0.302	8.4%	9.74	439	0.307	4.8%	10.03	446	0.302	0.9%
				9.87	442	0.402	4.7%	10.03	442	0.406	1.0%
				9.87	440	0.49	4.7%	9.91	450	0.498	1.2%
9.79	595	0.299	8.2%	9.71	572	0.300	3.7%	10.12	580	0.302	1.1%
				9.72	572	0.403	3.7%	10.07	584	0.396	1.2%
9.99	576	0.407	7.8%	9.60	574	0.511	3.8%	10.00	589	0.507	1.2%

Pressure losses for the medium and high MFR injectors were generally acceptable. For the low MFR configuration, the higher pressure loss is mainly attributed to the high velocity within

the air gate, and the fact that the air gate length was extended from 5mm (design) to 19mm (for powder removal). The actual pressure loss for this design was tripled compared to CFD predictions with a 5mm air gate.

4.3.4 NO_x Results

NO_x emissions for different engines and different operating conditions are currently compared on a basis of:

1. Mass of NO_x per unit thrust (Dp/Foo – g/kN)(used to quantify NO_x in the Landing and Take-Off (LTO) cycle for engine certification)
2. Emissions Index (EINO_x – g/kg of fuel)

These metrics are used for current legislation and published in the ICAO Engine Emissions Database. Since all current engines use Jet A-1 as fuel, these metrics provide a fair basis for comparison. However, EINO_x is not suitable for NO_x comparisons between engines operating on different fuels (particularly when comparing Jet A-1 with hydrogen) due to the significant difference in the Lower Heating Values (LHV) between the fuels: 43MJ/kg of Jet A-1 compared to 120MJ/kg of hydrogen.

Thus, a more appropriate metric for comparison would be an energy-based emission index (EEINO_x – g/MJ). EINO_x for a specific fuel can be converted to EEINO_x by Equation 7

$$EEINO_x = \frac{EINO_x}{LHV} \quad \text{Equation 7}$$

Where LHV is the lower heating value of the fuel in MJ/kg. EEINO_x is used here for the presentation of the results of both the experimental campaign and the numerical simulations to allow a fair basis of comparison of the NO_x produced by Jet A-1 and H₂ fuelled engines.

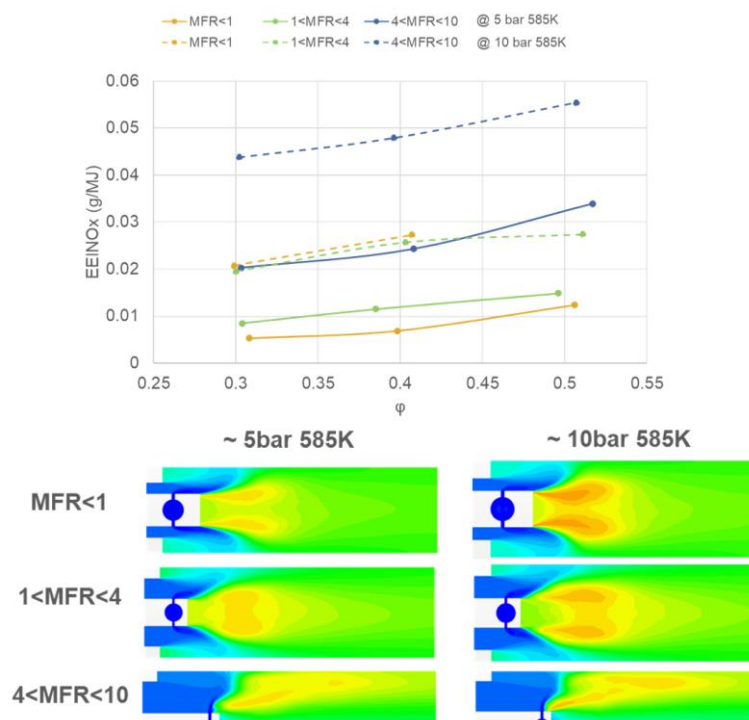


Figure 4-10: Top: EEINOx comparisons (experimental) for the three injector designs as a function of inlet pressure, inlet temperature and equivalence ratio. Bottom: Corresponding numerical simulations illustrating temperature contours.

Of all the tested cases, the low and medium momentum flux ratio injectors show significantly lower NOx than the high momentum flux ratio configuration. Referring to Figure 4-6, low and mid MFR configurations are situated on the left of point B. Based on the corresponding LES results presented in Figure 4-10, it can be seen that the flames are generally short with low residence time. The flames are located near or within the inner recirculation zone so that the flame-flame interaction is limited. However, for the higher MFR design, the flames are longer and merge with the neighbouring flames (represented by periodic boundary).

There exist uncertainties between the predicted position (i.e., the MFR) for the transition points A and B by CFD and the corresponding experimental values. The medium MFR design was predicted to be near the local maxima (point A), whereas according to the NOx experimental results, it is more likely to be situated in the region between point A and B. The low MFR design is on the other hand closer to the local maxima (point A) than predicted.

The main challenges with numerical modelling, even with LES, is to predict more accurately the locations of the transition points identified above, which are essential in identifying low NOx designs (without the need for the more costly experiments). The NOx trends predictions are also highly sensitive to these locations. Tuning numerical models for hydrogen combustion will require good calibration for physical properties such as diffusivity, as well as capturing temperature distributions and heat losses that are representative of the experimental set up. Flame imaging is essential in providing detailed information for this. Therefore, despite its high cost and challenges when implemented for a high-pressure high-temperature combustion rig, it is strongly recommended for any future experiments.

In order to provide an idea of how hydrogen compares to Jet A-1 at similar operating conditions, the experimental results were compared to the EEINOx produced by a

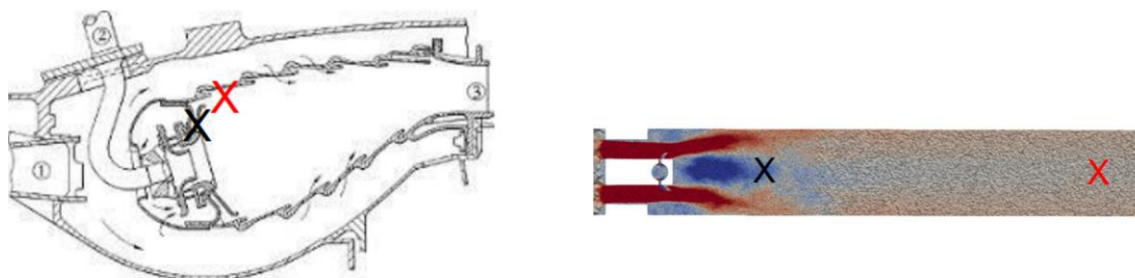
LEAP1A35A engine (currently in service) at 7% Landing and Take-Off (LTO) Thrust. The 7% LTO thrust point was chosen because the combustor inlet pressure (P_3) and air-inlet temperature (T_3) are approximately 8bar and 550K respectively. The condition is close to those of the experimental tests performed for hydrogen micromix combustion. The EINO_x value was extracted from the ICAO emissions database and the EEINO_x was then calculated, which is approximately 0.11.

Except for one test point, for the high MFR design, for similar combustor inlet conditions, the hydrogen micromix combustion system produces at least 50% lower NO_x than the SOA Jet A-1 combustion system. It is therefore recommended that the H₂ micromix injectors are designed with lower momentum flux ratios.

4.4 Altitude Relight Performance Simulations

High fidelity simulations were run of the micromix injector system in order to simulate high altitude relight, an important requirement for combustion systems in aircraft. The study explored the effects of altitude and fuel equivalence ratio on relight performance.

The velocity field and recirculation zone from the pre-ignition simulations showed that the ignition needs to be placed very close (a few millimetres) downstream of the injector, marked as the black cross in Figure 4-11, instead of further downstream as for conventional combustors (red cross). There could potentially be difficulties in integrating such an ignition source, as well as challenges in durability of the combustor components due to the very short distance to the ignition source.



Source: Gleason and Bahr (1979)

Figure 4-11: Ignition source positioning in a conventional combustor (left) and in a micromix combustion domain (right). The red and black crosses compare the ignition source locations for Jet A-1 (conventional combustor) and a hydrogen (micromix combustor) respectively.

The simulations at low altitude and equivalence ratio of 0.4 show no issue in relight as the ignition is sufficiently close to the injector. At high altitude with an equivalence ratio of 0.4, the relight is much more difficult and time consuming. A single spark was not sufficient to light the domain and the spark had to be repetitively fired to sustain combustion. In this case the hydrogen consumption speed was lower relative to the lower-altitude case, so the flame struggled to move upstream to the inner recirculation zone where it is supposed to stabilise as shown in Figure 4-12.

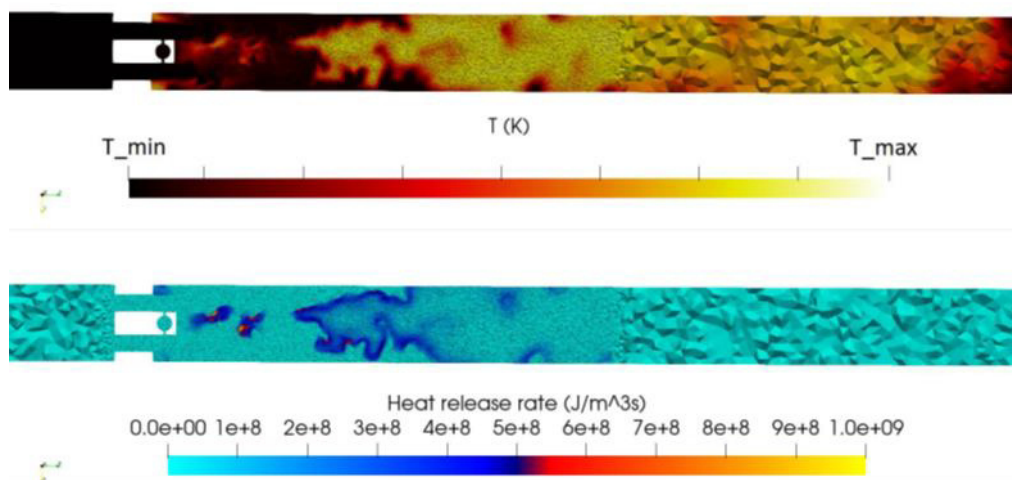


Figure 4-12: The flow temperature (normalised) and heat release rate for the high-altitude case at $t=3ms$ after ignition ($\phi=0.4$)

The effect of increasing the equivalence ratio from 0.4 to 1.0 had a significant impact on the relight performance, as the flame was easily ignited and stabilized in the recirculation zone after a single spark, as illustrated in Figure 4-13. This is due to the combined impact of the increased flame speed at higher equivalence ratio as well as the increased momentum flux ratio, which significantly increased the size of recirculation zone.

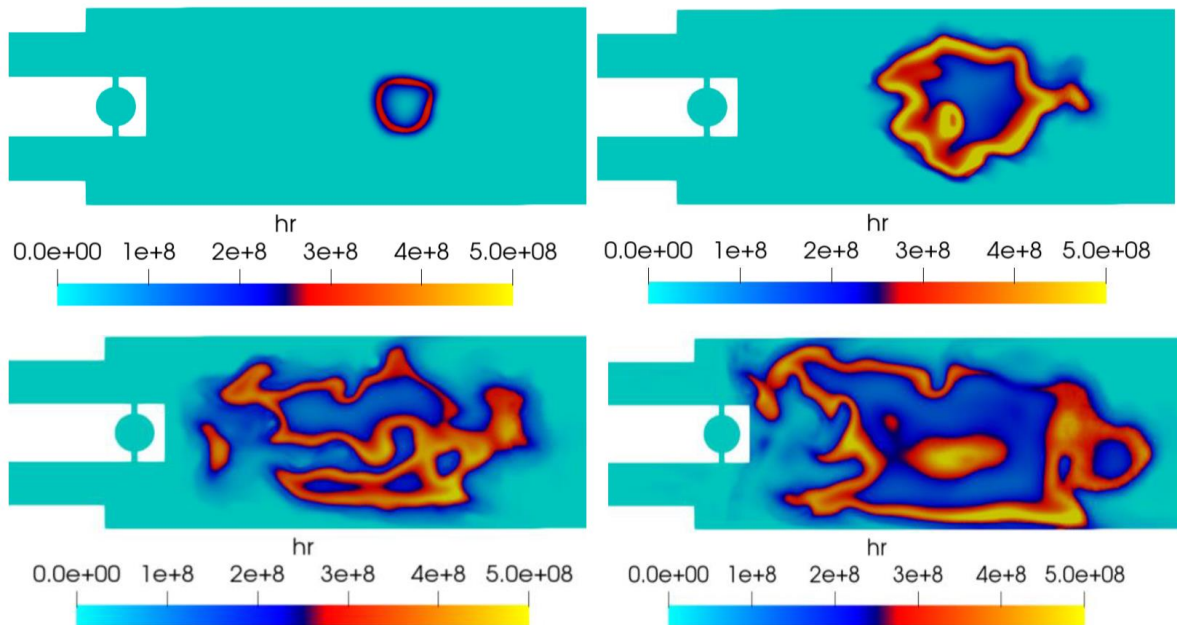


Figure 4-13: The heat release during ignition at $t=0s$, $t=0.3ms$, $t=0.7ms$ and $t=1ms$ ($\phi=1$ - stoichiometric)

For a micromix injector, the effect of equivalence ratio (which influences the momentum flux ratio) is the key feature that influences the performance of the combustor. This allows operational flexibility (particularly for challenging operating conditions e.g., altitude relight) without the complexity associated with variable geometry combustor designs. At the high altitude relight condition, increased jet penetration (at a higher equivalence ratio) ensures high flame speed and large recirculation zones for good ignition performance. At high power conditions, a low momentum flux ratio limits the interaction of flames and the combustion residence time and hence limits NO_x production. With an appropriate fuel staging strategy, both low emissions and operability requirements could be achieved.

5 H₂ Micromix Combustor Preliminary Sizing, General Arrangement and Emissions Analyses

5.1 Aim of H₂ Micromix Combustor Preliminary Sizing

The purpose of the H₂ micromix combustor preliminary design and sizing task was two-fold.

1. The primary goal of the task was to establish a methodology for sizing a novel hydrogen micromix combustor design.
2. The secondary objective of the task was to determine the appropriate size for a representative H₂ micromix combustor for a high bypass ratio turbofan engine, for the ENABLEH2 Year 2050 blended wing body long-range aircraft (LR BWB 2050)[2] and to derive a lower-order NO_x emissions prediction correlation for the mission-level NO_x assessments.

5.2 Hydrogen Micromix Combustor Architecture

For the conceptual H₂ micromix combustor, the following assumptions and design choices were made based on the best engineering judgements. These assumptions primarily relate to the combustor architecture.

- In the preliminary design phase, the H₂ Micromix combustor was designed without primary, secondary, or dilution holes. Conventional combustors employ primary and secondary air jets to enhance flow recirculation to stabilize the flame and completely combust the unburnt hydrocarbons. However, this is not necessary in the H₂ Micromix combustor. The temperature profile can be regulated through active fuel scheduling.
- In the near future, high-temperature-resistant materials such as Ceramic Matrix Composites (CMCs) will be used in liners, as evidenced by GE's TAPS-III [7] and Rolls-Royce's Phase 5 combustors, which have implemented CMCs and tiled walls[8]. Furthermore, improvements in cooling technology such as enhanced impingement-effusion cooling are expected to decrease the cooling air requirement.
- The primary purpose of air entering the liner is for lean H₂ combustion. A small fraction of this air will be utilized for cooling the mating surface between the liner and injector plate, which will be introduced into the combustor through cooling jets from the top and bottom unfuelled air gates. This will provide protection to the liner surface in the primary zone, where the highest temperatures are anticipated. Downstream the air will mix with the combustion products, leading to a reduction in the equivalence ratio in the combustor.

5.3 Preliminary Combustor Design and Sizing

In the preliminary combustor sizing stage, the focus is on determining the dimensions of the aerodynamic components of the combustor (casing and liner). The sizing process typically involves utilizing empirical equations and coefficients that have been established through experimental work. This approach allows for a rapid completion of a preliminary design with a reasonable level of accuracy, which can then be further refined through more resource-intensive high-fidelity numerical simulations. The velocity method described in Ref. [9] and [10] was chosen for this work for the following reasons:

- The pressure loss method [11] and chemical reaction rate method [12] both rely on empirical and semi-empirical correlations and coefficients that have been developed for specific Jet A-1 combustors. As such, it is not appropriate to apply these methods for preliminary design of H₂ micromix combustor.
- The velocity method was used as it allows for the selection of a liner velocity that is suitable for the flow requirements of the chosen micromix injector design. The velocity selection was based on numerical studies that focused on achieving good ignition, flame stability, and low NO_x [3], [5], [13].

5.3.1 H₂ Micromix Combustor Design and Sizing Methodology

The H₂ micromix combustor 1-D aerodynamic design and sizing methodology comprised two processes:

1. The first step involved calculating the geometric parameters for the liner and casing based on the combustor inlet boundary conditions and geometric constraints obtained from the engine performance simulation data.
2. In the second step, the number and distribution of the H₂ micromix injectors were established for a given micromix injector geometry.

5.3.2 Assumptions

For the preliminary sizing several assumptions were made particularly with respect to materials and cooling technologies for the combustor liner. The implications of these assumptions require further experimental validation. This was beyond the scope of ENABLEH2.

5.3.2.1 Air Distribution

By Y2050 advanced CMC liner materials are expected to be available which will significantly reduce the liner cooling flows, although it seems unlikely that combustor walls would be completely uncooled. Some air will also be required for high pressure turbine nozzle guide vane film cooling. Hence, it is assumed approximately 10% of combustor inlet flow will be cooling flows and remaining 90% will contribute to combustion. A schematic of the H₂ micromix combustor is shown in Figure 5-1.

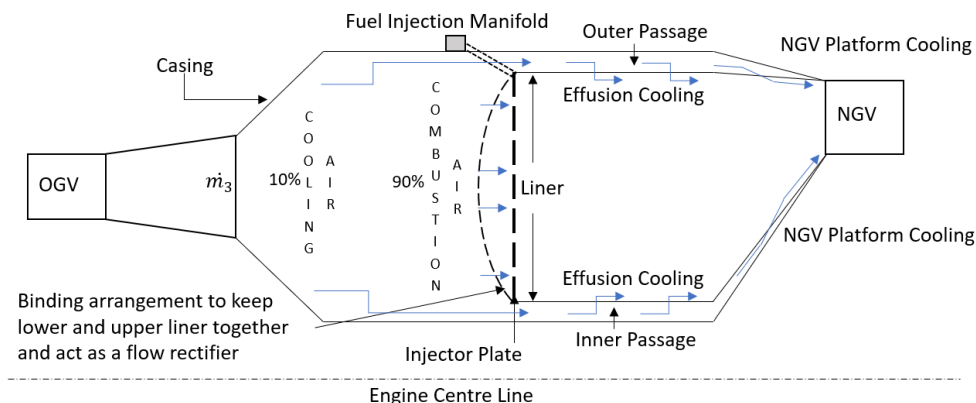


Figure 5-1: Conceptual schematic of H₂ micromix combustor illustrating air-flows

5.3.2.2 Flow Velocities

Velocity ranges of 7-12 m/s for the liner and 35-60 m/s for the passage have been recommended for Jet A-1 fuelled combustors [9], [10]. However, as stated in Section 5.3, the flow velocity for the H₂ micromix combustor liner was deduced based on the flow requirements downstream of the airgate based on the single-injector numerical studies presented in Section 4 and published in Ref. [3], [5]. The liner flow velocity of 15m/s was chosen.

The use of advanced high temperature materials such as CMCs is projected for combustor liners. Therefore, conventional film cooling techniques can be replaced with enhanced impingement-effusion cooling for the liner. As a result, a relatively low cooling flow velocity of 30m/s was assumed to improve effusion cooling efficiency.

5.3.2.3 Flow Rectification

Conventional Jet A-1 combustors feature a curved dome with a snout that conditions the flow entering the injector. In contrast, the H₂ micromix combustor utilizes a flat injector plate mounted on a flat liner front as shown in Figure 5-1 to facilitate manufacturing and integration. Without the traditional dome and snout arrangement, the H₂ micromix combustor requires a flow rectifying arrangement. A proposed solution is to use a porous medium as a flow rectifier downstream of the diffuser and upstream of the liner front for example as shown in Figure 5-2 described in the patent by Horikawa et al.[14]. This was beyond the scope of the ENABLEH2, and hence a detailed analysis was not undertaken to verify the efficacy of this arrangement.

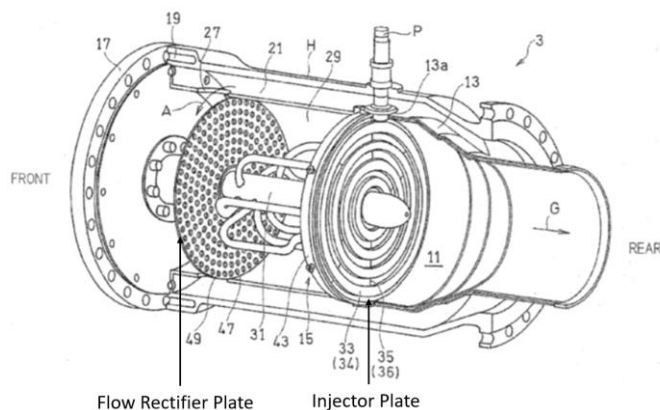


Figure 5-2: Example of a flow rectifier for a H₂ micromix combustor[14]

5.3.3 Combustor Component Sizing

Figure 5-3 presents the methodology for the preliminary aerodynamic sizing of the liner and casing of the H₂ micromix combustor. The sizing methodology used in this study is adapted from the Lean Partially Premixed (LPP) combustor sizing approach described by Yize et al. [10] and Mavris [12]. The proposed methodology accounts for the inlet boundary flow conditions and geometric constraints as inputs and calculates the combustor liner and casing dimensions based on the air split and flow velocities. The combustor's tilt angle, denoted by α (refer to Figure 5-3), is assumed to remain constant from station 3 to station 4, as the combustor may be angled from the diffuser inlet to the transition duct exit at the NGV. To obtain the complete geometry, each point is parameterized by α , and the liner and casing areas are assumed to be constant. However, the liner height varies based on the mean radius of each station. To ensure that the exit mean radius matches the NGV pitch radius, the angle α is adjusted in the solver.

Finally, the required Energy Density (ED) of the combustor is calculated using Equation 8. This defines the minimum required ED for a given liner area.

$$ED \left(\frac{MW}{m^2 * Bar} \right) = \frac{E_{DP}}{A_{Liner} * P_{DP}} = \frac{\dot{m}_{fuel} * LHV}{A_{Liner} * P_{DP}} \quad \text{Equation 8}$$

Where:

E_{DP} is the energy released at engine design point (MW),

\dot{m}_{fuel} is the fuel flow at engine design point (kg/s),

LHV is the lower heating value of fuel (MJ/kg),

A_{Liner} is the area of a liner (m²),

P_{DP} is the combustion chamber pressure at engine design point (bar)

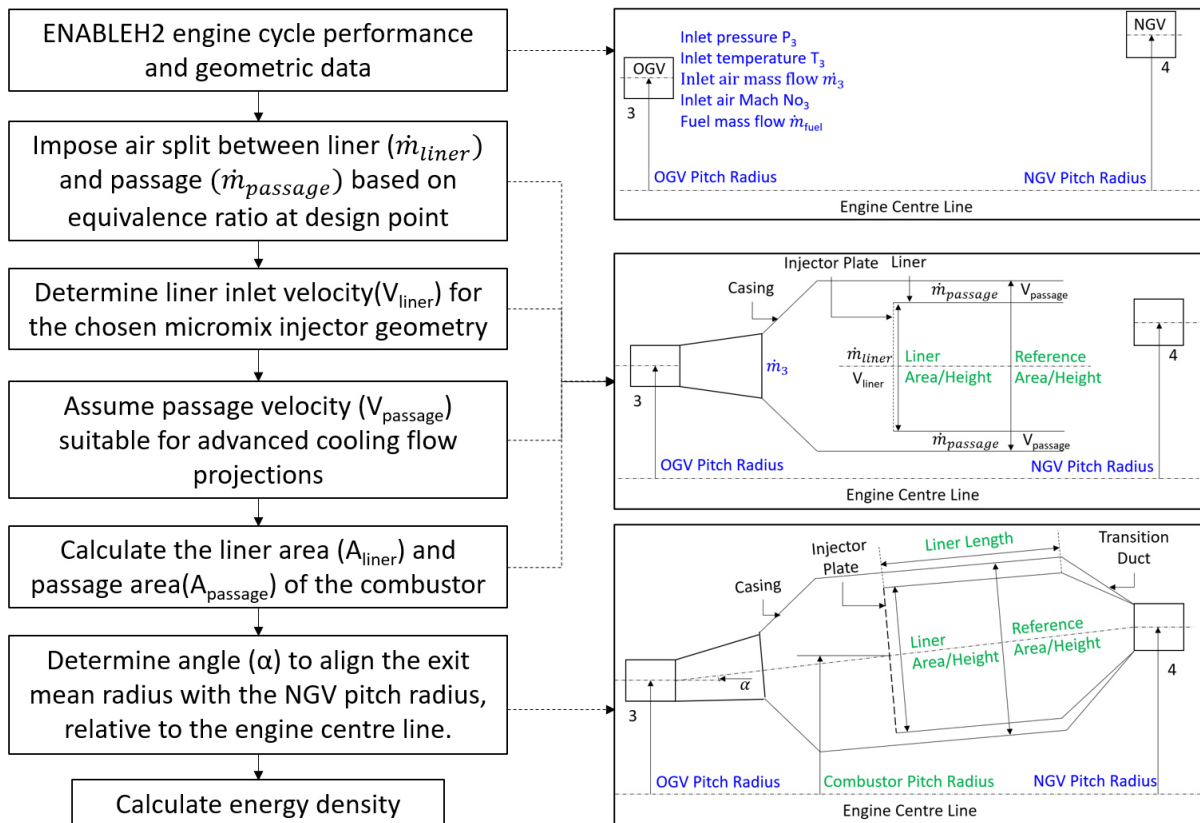


Figure 5-3: H₂ micromix combustor aerodynamic sizing methodology

The outcome of the sizing task is shown in Figure 5-4.

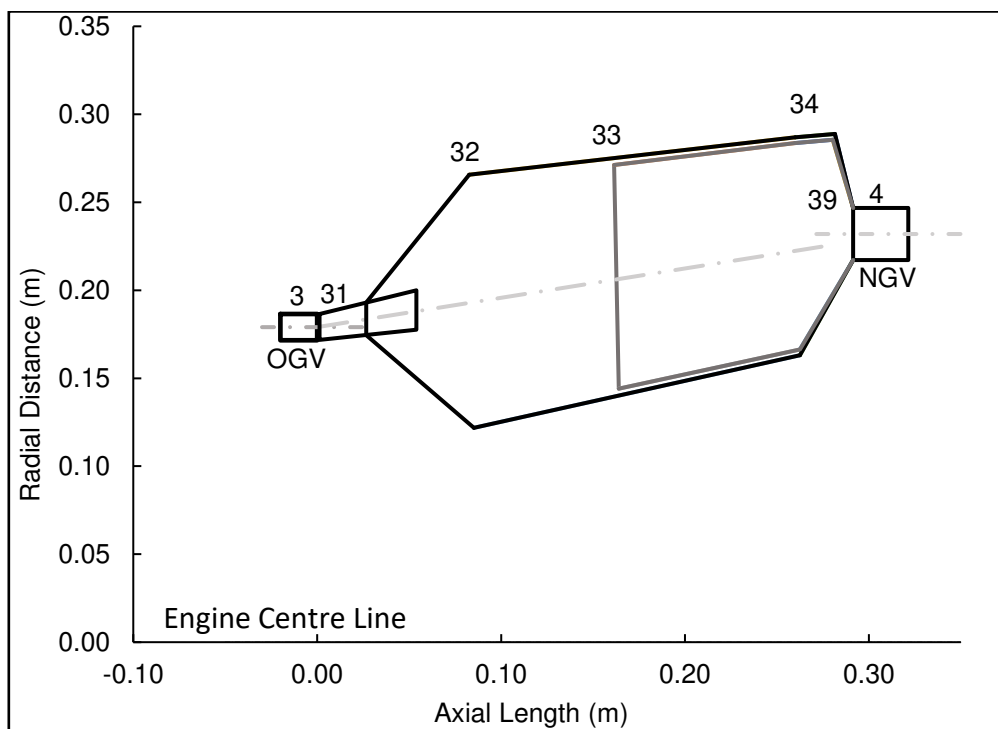


Figure 5-4: Preliminary general arrangement of the H₂ micromix combustor

5.4 H₂ Micromix Injector Array Design

The H₂ micromix combustor comprises an array of injectors arranged on an injector plate, with a flat front liner modelled as shown in Figure 5-1 and Figure 5-4. The selected injector geometry, as presented in Table 5-1, was derived from the single injector numerical studies. It is a design that delivered the lowest NO_x emissions among the injector geometries evaluated in Section 4.2 and published in Ref. [3], [5], [13], [15], [16].

Table 5-1: Chosen H₂ micromix injector geometry


Shape	Air Gate Diameter (mm)	Air Gate Height (mm)	Aspect Ratio (AR)	H ₂ Injection Orifice Diameter(mm)	Momentum Flux Ratio
	2.11	1.055	0.5	0.3	0.5-0.55

Figure 5-5 presents an iterative methodology for distributing a selected micromix injector geometry onto the liner front of a combustor. This process involves calculating the geometric parameters and flow conditions through the geometry in the first step and iterating until the pressure-drop meets the targeted levels. Isentropic flow equations are then used to determine the flow conditions through the airgate and hydrogen injection orifice, enabling calculation of the Momentum MFR. The energy density of the injector element is then compared with the required energy density of the combustor. Through the design iterations following constraints were imposed:

1. Energy Density
2. Momentum Flux ratio
3. Pressure Loss across Injector plate (air gate channel)

Table 5-2: Target values of the key variable for the preferred injector geometry

JIC Parameters	Values
MFR	0.50-0.55
Energy Density ED (MW/m ² -bar)	6.67
Pressure Loss (through air gate)	2.5%

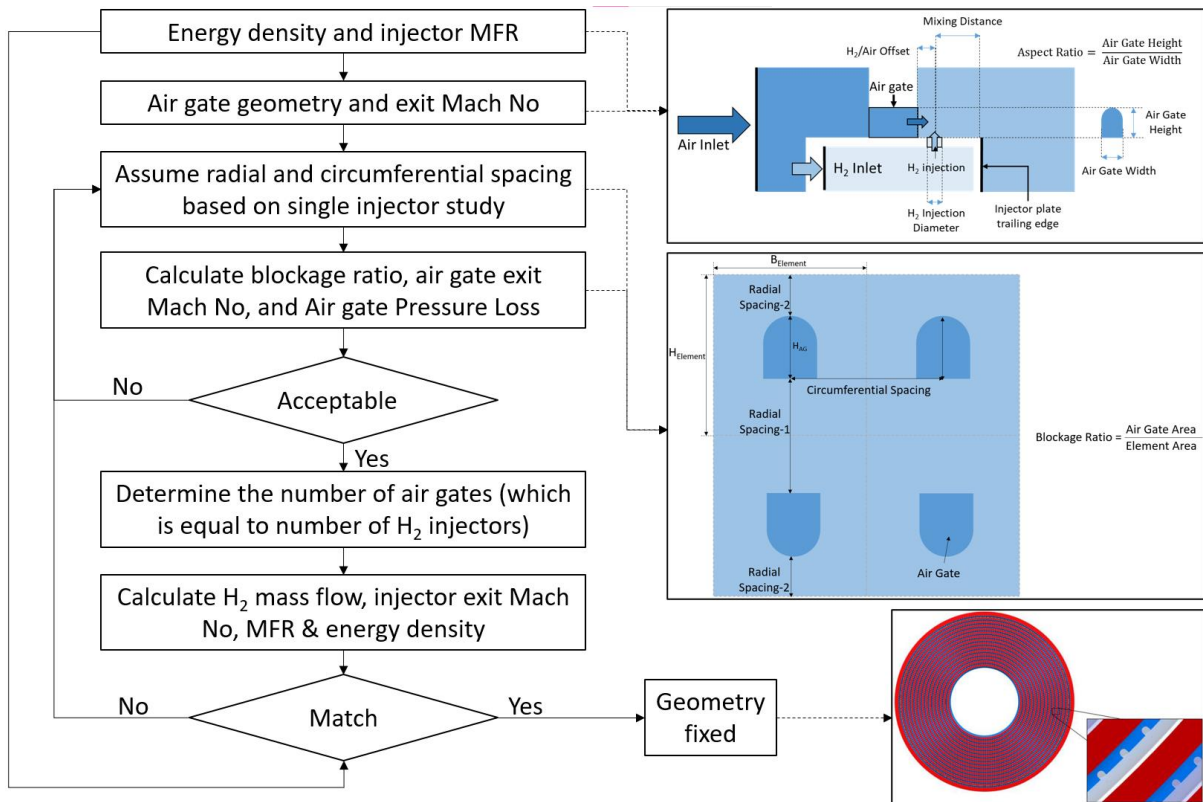


Figure 5-5: H₂ micromix combustor injector array distribution methodology (images adapted from [3], [5])

The outcome of the injector array distribution is shown in Table 5-3.

Table 5-3: Micromix injector array distribution results

Radial Spacing-1 (mm)	Radial Spacing-2 (mm)	Circumferential Spacing (mm)	Airgate PL (%)	MFR	Number of Injectors	Energy Density (MW/m ² -Bar)
3.0	1.445	3.8	2.4	0.5	11124	6.67

5.5 Implementation

The novel design of the hydrogen micromix combustor is a result of the integration of knowledge obtained from previous works and ongoing research [3], [17], [18]. The implementation of a new micromixer injector geometry involves positioning a substantial number of injectors on the liner face which brings about most of the radical changes to the conventional combustor design. The schematic representation of the hydrogen micromix combustor is presented in Figure 5-6. The burner stem may contain up to three separate hydrogen channels to facilitate staged combustion to minimise the NOx by optimising local FAR and MFR at various power settings. Furthermore, the inner and outer liners may be joined at a specific area located at the front between the burner stems. This connection serves to reinforce the structural integrity of the combustor and ensures proper functioning. Note the connections and seals of the burner-head manifold have been omitted for clarity.

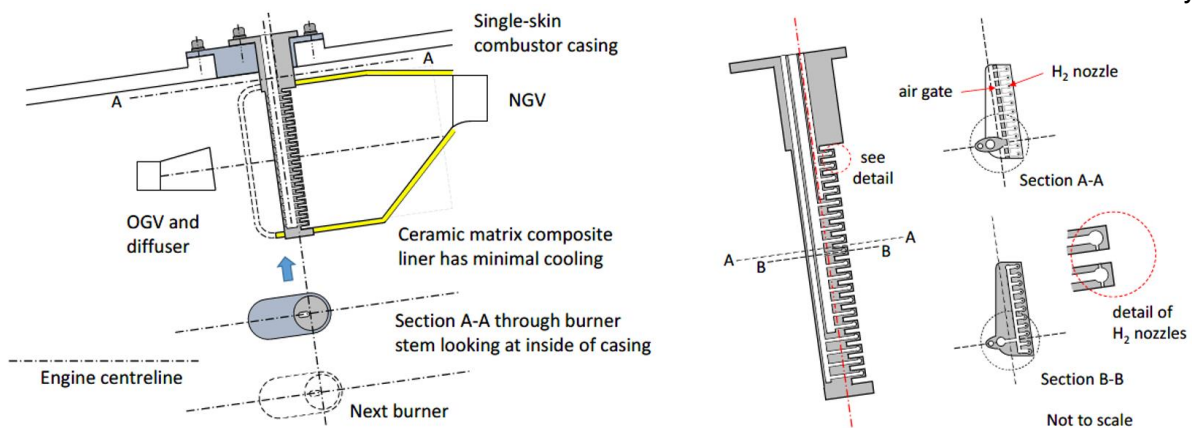


Figure 5-6: H₂ micromix combustor schematic cross-section with burner in its working position

The integration of the burner segment in the combustor is shown in Figure 5-7, this configuration necessitates a 90° rotation of the burners prior to extraction. In this example there are 24 burners, each providing a 15° injector plate segment. While it is possible to reduce the number of burners, this would result in an increase in the length of the openings in the combustor casing, which could impact the structural integrity of the engine.

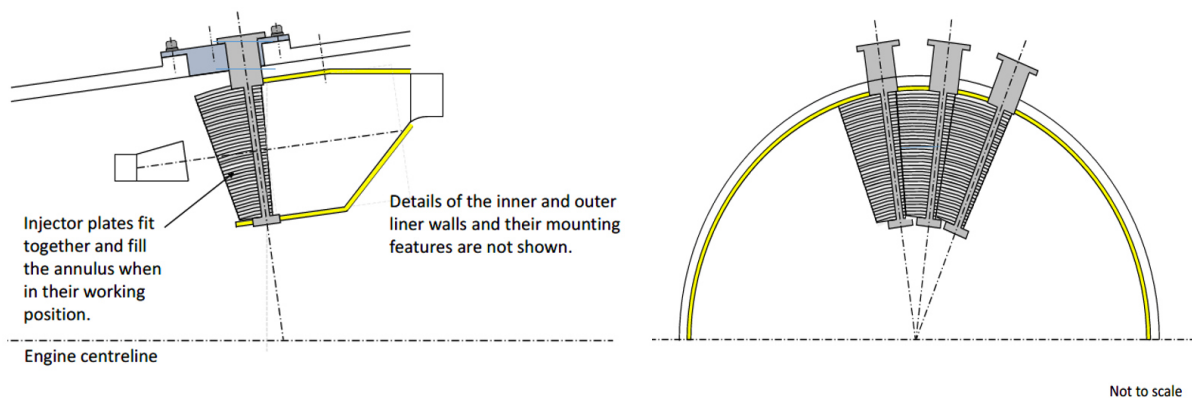


Figure 5-7: H₂ micromix combustor cross-section with burner rotated ready for removal and three segments installed.

The success of hydrogen combustor sizing relies on achieving the ultra-low NO_x potential of hydrogen micro mixing. Therefore, it is desirable to evaluate the NO_x emissions of the sized combustor at the preliminary stage. A dedicated NO_x emissions prediction model was developed for the preliminary evaluation of a hydrogen combustor's NO_x emissions as no such models were available in the public domain at the time of publication.

5.6 NOx Emissions Assessment

To evaluate NO_x emissions of a hydrogen micromix combustor in the preliminary stage, a lower order NO_x emission prediction model for H₂ micromix combustion system was developed as an alternative to high-fidelity numerical simulations, which are not practical due to their high time and cost requirements. This section discusses the LTO cycle legislation, the requirements of the model and then elaborates the development methodology.

5.6.1 Landing and Take-off (LTO) Cycle

The Committee on Aviation Environmental Protection (CAEP), a body of International Civil Aviation Organisation (ICAO), has formulated “Annex 16: Environmental Protection, Volume 2: Aircraft Engine Emissions to the Convention on International Civil Aviation” which sets the rules and regulations which should be followed by all aircraft engine makers concerning emission measurements and certification. Emissions currently are regulated for Landing-Take Off (LTO) cycles and an LTO cycle comprises the standard thrust specifications and durations shown in Figure 5-8.

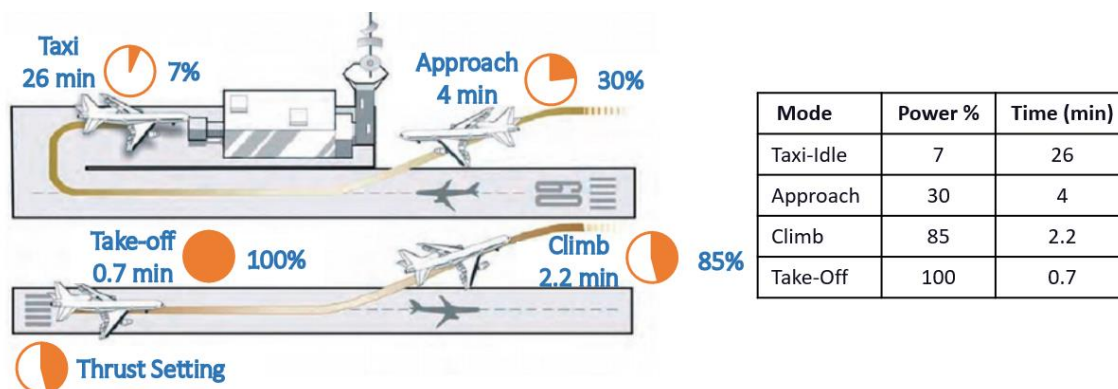


Figure 5-8: LTO Cycle with power settings and durations for emission measurements [19]

It should be noted that while all measurements are made at sea-level static conditions, they are representative of thrust settings and durations for the four LTO conditions (taxi, take-off, climb and approach). These regulations are considered representative for civil subsonic turbofan/turbojet engines with rated thrust levels above 26.7 kN and up to an altitude of 3000 feet.

5.6.2 Lower Order NOx Emissions Prediction Model

A lower order emissions prediction model can guide technological improvements at the preliminary design stage. They allow for rapid design space exploration thereby significantly reducing risk and costs by identifying specific designs that merit further higher-fidelity modelling and experimental development. This reduces development costs and helps to accelerate entry into the service of low-emissions combustion technologies.

Additionally, the lower order model is more suitable for Techno-Economic Environmental Risk Assessment (TERA) type studies, which comprise aircraft mission-level design space exploration and multi-disciplinary optimization studies. Due to their relatively lower computational cost, lower order models are better suited for these studies than the more computationally expensive, higher fidelity computational fluid dynamics (CFD) models.

The desired attributes of a lower order emissions prediction model are:

1. It should be simple to use with initially available preliminary engine-cycle design data (e.g., combustor inlet and outlet geometrical parameters and engine cycle performance data). It should also reasonably apply to novel designs for which rig data is not available and continuously refined based on any data generated from subsequent experimental/numerical campaigns.
2. It should not require excessive computational time so that they may be used for rigorous design space exploration, comprising parametric and optimisation (and trade-off) analyses.
3. It should be adequately verified/validated (either absolute values or trends, depending on the data available) to provide a good indication of the reliability/fidelity of the results.
4. It should apply to the whole aircraft mission profile to evaluate both LTO and mission NO_x.

It is difficult to have a model that will meet all the requirements as stated above and hence the selection of the best-suited model always has some trade-off considerations. These trade-offs are mostly specific to the application requirement and the stage of the design process.

5.6.3 NO_x Emissions Prediction Correlation Development Methodology

Correlation-based models are derived from either experimental data or engine data. In absence of experimental or engine data, the numerical campaign was run over a wide range of parametric values covering a typical aircraft mission profile Idle, End of Runway (EoR), Top of Climb (ToC), and Cruise.

The numerical simulations comprised two campaigns:

The first campaign assessed the combined variation of equivalence ratio, combustor inlet temperature, and pressure representative of the aircraft mission profile. This was repeated for multiple-step changes in all the parameters.

In the second campaign an individual parameter (combustor inlet temperature) was varied while keeping all other boundary conditions the same again repeating for multiple-step changes. The database was then created from these simulations and split into training data (80%) and numerical test data (20%). The NO_x correlation was then derived using the regression in python and “Generalised Reduced Gradient (GRG) Non-Linear (multi-start)” solver in MS Excel. The developed correlation was verified against the test data. The numerical simulations were conducted assuming the composition of dry air and the resulting correlation for EINO_x was subsequently corrected assuming 60% relative humidity at SLS conditions. The methodology adopted is shown in Figure 5-9.

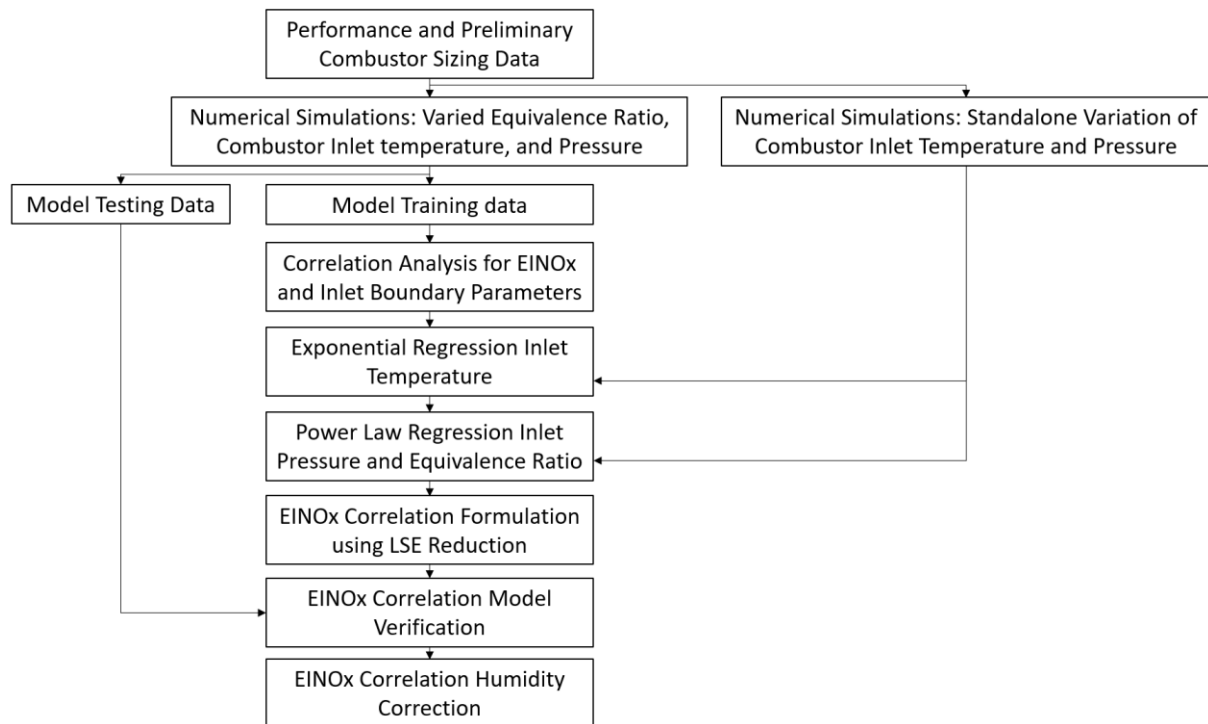


Figure 5-9: EINOX correlation development methodology

5.7 Numerical Setup

The geometry shown in Table 5-3 was arranged in an array of 24x2 matrix with twelve pairs of injectors in radial direction arranged in two columns i.e., 48 fuelled injectors. There are further 4 air gates that were not fuelled (two at the bottom of geometry in “Main 1” and two at the top of the geometry in “Main 2”) as shown in Figure 5-10. These serve as passages for film cooling air that does not contribute to combustion.

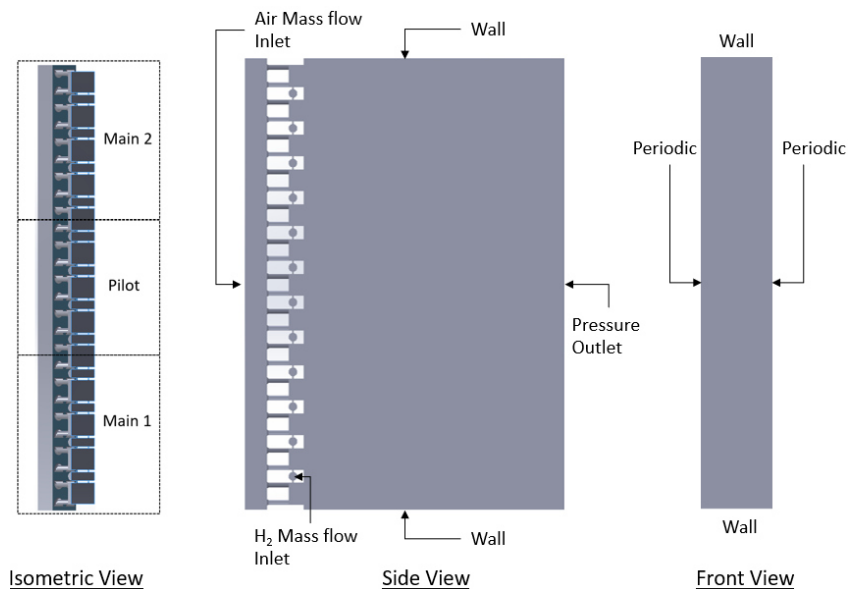


Figure 5-10: Numerical domain with staging

Table 5-4: Inlet boundary conditions used for numerical simulation campaign.

Pressure (kPa)	Temperatures (K)	Equivalence Ratio	Pilot Injector lit	Main 1 Injector Lit	Main 2 Injector Lit
395	446	0.13 to 0.20	Yes	No	No
397	546	0.13 to 0.20	Yes	No	No
1497	646	0.19 to 0.28	Yes	Yes	No
1501	746	0.19 to 0.28	Yes	Yes	No
2491	646	0.19 to 0.30	Yes	Yes	Yes
2496	746	0.19 to 0.30	Yes	Yes	Yes
3549	646	0.25 to 0.31	Yes	Yes	Yes
3556	746	0.25 to 0.31	Yes	Yes	Yes
4028	846	0.22 to 0.31	Yes	Yes	Yes
4036	946	0.22 to 0.31	Yes	Yes	Yes
6230	896	0.28 to 0.32	Yes	Yes	Yes
6240	996	0.28 to 0.32	Yes	Yes	Yes

The boundaries for H_2 and the air inlet were set as “mass flow inlet”. Periodic interface boundary conditions were used to represent the circumferential distribution of the injectors. The exit of the domain was set to a pressure outlet. For all the cases the hydrogen fuel injection temperature was set at 450K, and the air inlet conditions (temperatures and pressures), and equivalence ratios shown in Table 5-4.

For fuel staging, the centre 16 injector were assigned as pilots, the 16 closest to the shaft were designated “Main 1” while the 16 farthest from the shaft designated “Main 2”. The conceptual fuel staging is shown in Figure 5-11, the key criterion in staging was to keep the pilot injectors at an equivalence ratio of 0.40 for all power conditions to ensure flame stability. At the lowest power condition all the fuel was directed to the pilot only ($m_{fuel\ Pilot}$), while for all other power conditions any remaining fuel was distributed to the Main injectors ($m_{fuel\ Main}$). The pattern of injectors that were lit is shown in Table 5-4.

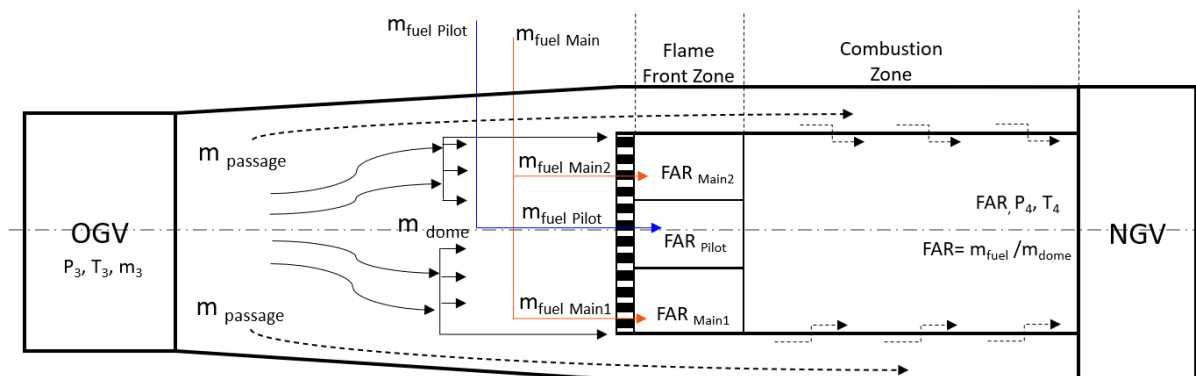


Figure 5-11: Air and Fuel Staging Strategy

Three-dimensional steady Reynolds Averaged Navier Stokes (RANS) analysis was performed for all the cases using STAR-CCM+. The numerical setup is explained in Section 4.

5.8 Numerical Simulation Results

Figure 5-12 shows the effect of simultaneous variation of equivalence ratio, combustor inlet temperature, and pressure on NO_x emissions at different engine power settings. The results follow the expected trends i.e., NO_x emissions increase with increasing equivalence ratio, combustor inlet temperature, and pressure [20]–[23]. The trends highlight certain observation listed below-

1. For the range of conditions that were numerically investigated as shown in Table 5-4 the NO_x emissions have an exponential dependence on the flame temperature in the combustion zone in the combustor.
2. The influence of pressure is more significant at higher equivalence ratio.

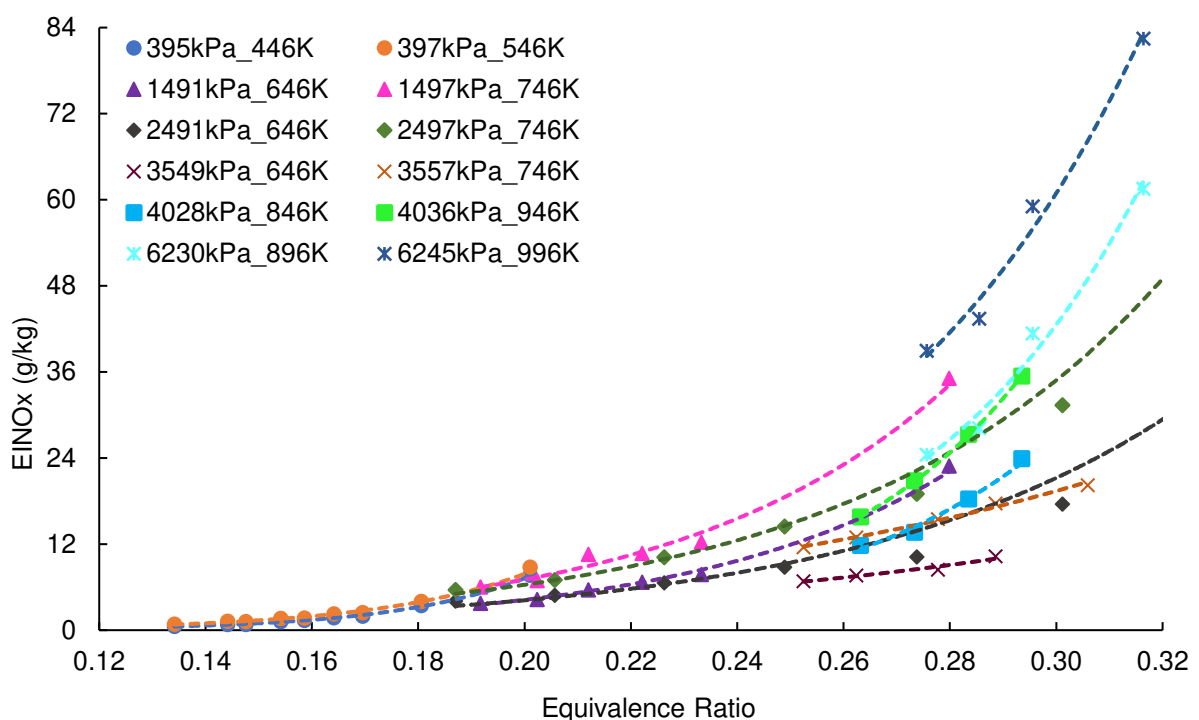


Figure 5-12: *EINO_x as a function of equivalence ratio for range of operating conditions*

5.8.1 Influence of Pressure

For a given temperature, the relationship between EINO_x and pressure is a power law function as shown in Figure 5-13. This is consistent with the findings of Kroniger et al. [22], [23] for hydrogen fuel. The relation shown in Equation 9 was derived.

$$EINO_x \propto f(P_3^x) \quad \text{Equation 9}$$

Where x is the exponent coefficient of pressure

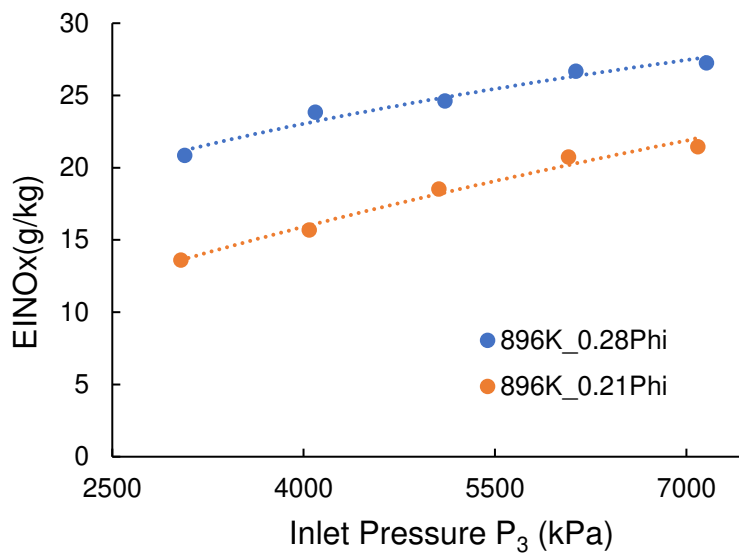


Figure 5-13: Influence of inlet pressure on EINO_x at constant temperature and equivalence ratio

5.8.2 Influence of Temperature

For a given pressure, EINO_x increases exponentially as a function of inlet temperature, as shown in Figure 5-14, this is consistent with the studies. The relation shown in Equation 10 was derived.

$$EINO_x \propto f(e^{T_3 \cdot y}) \tag{Equation 10}$$

Where y is the temperature exponential coefficient

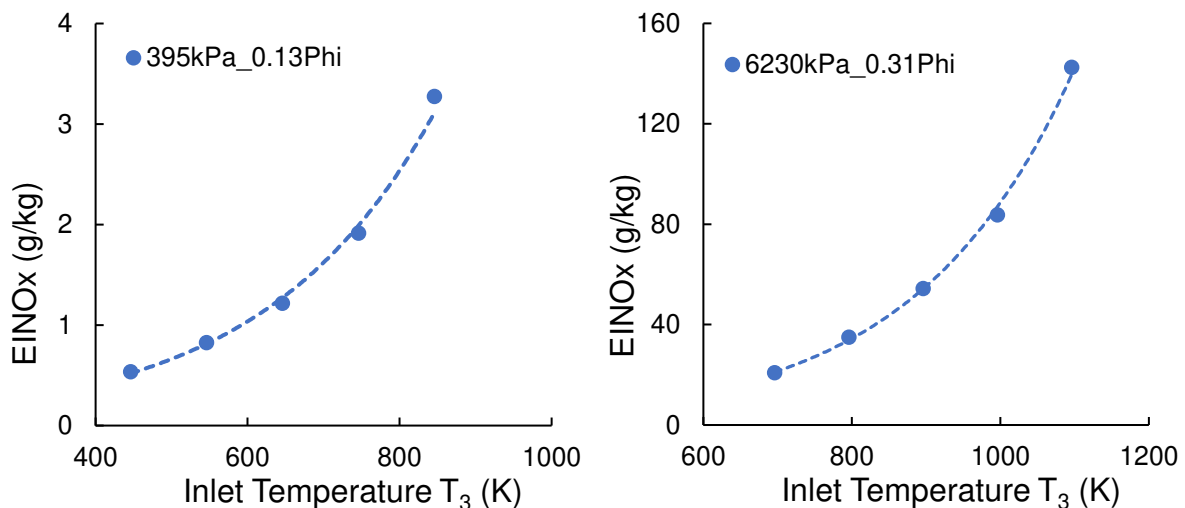


Figure 5-14: Influence of inlet temperature on EINO_x at constant pressure and equivalence ratio

5.9 NOx Correlation

NOx emissions formation typically depends on cycle parameters (inlet pressure, inlet temperature, combustion zone equivalence ratio, outlet temperature, and fuel composition), design choices (e.g., degree of premixing, fuel injector and swirler design, fuel staging strategy) and performance requirements.

For preliminary NOx estimations, general industry practise is to derive NOx emissions prediction correlations based on the engine cycle parameters that are typically available from engine cycle performance and preliminary sizing data. At the detailed design stage, the correlations are then refined using more precise performance and sizing data before being fully validated during subsequent experimental campaigns.

5.9.1 NOx Emissions Prediction Correlation Variables

For a typical gas turbine combustors thermal NOx emissions are a function of flame temperature (linked to the reaction rate), residence time and mixing homogeneity.

NOx emissions can therefore be derived as a function of the variables shown in Equation 11 which influence the mixing homogeneity, reaction rate and residence time.

$$NOx = f (P_3, T_3, \Delta P_{fa}, \Delta P_c, Geo, T_{ad}, T_4) \quad \text{Equation 11}$$

Where:

Geo is combustor geometry,

ΔP_{fa} is the fractional differential in pressure between the fuel and air,

ΔP_c is the combustor fractional pressure loss,

T_4 is the combustor outlet temperature,

P_3 is the combustor inlet pressure,

T_3 is the combustor inlet temperature,

T_{ad} is the combustor adiabatic flame temperature.

If the geometry and design of the combustor is fixed, then the simplified NOx correlation relating only to its inlet boundary conditions can be developed as shown in Equation 12.

$$NOx = f (P_3, T_3, T_4, T_{ad}) \quad \text{Equation 12}$$

However quite often when running an experimental campaign for deriving NOx emissions correlations some of this data may not be measurable (such as T_{ad}) or challenging and costly to measure (such as T_4). NOx emissions may be therefore correlated to other parameters that can be measured in the rig such as FAR or equivalence ratio [21], [24]–[27] which implicitly capture the effect of the variables T_{ad} and T_4 .

5.9.2 NOx Emissions Prediction Correlation

As presented in Section 5.8,

1. NOx emissions have an exponential dependence on temperature.
2. The relationship between EINOx and pressure is a power law function.

- The relationship between EINOx and equivalence ratio is a power law function.

Using these relationships, the correlation for EINOx described in Equation 13, was developed.

$$EINOx = a * P_3^b * e^{\frac{T_3}{c}} * \Phi^d \tag{Equation 13}$$

Where:

- a is the coefficient of proportionality,
- b is the combustor inlet pressure (P_3) exponent coefficient,
- c is the combustor inlet temperature (T_3) exponential coefficient,
- d is the combustor equivalence ratio (Φ) exponent coefficient.

First, the exponential coefficient of temperature “c” was obtained for a fixed pressure and equivalence ratio based on the dataset for standalone inlet temperature variation described in Section 5.8.2. Similarly, the coefficient “b” was derived using results from Section 5.8.1 accounting only for the pressure variation. Finally, the coefficient “d” was derived using the results from Section 5.8 varying both the combustor inlet temperature, and the pressure.

Next based on Equation 13, these coefficients were exported into MS Excel for correlation Least Square Error(LSE) reduction using the Generalised Reduced Gradient (GRG) Nonlinear with Multi-Start solver [28], [29]. The training dataset described in Section 5.6.3 and Table 5-4 was used. Numerical test data was randomly selected and excluded from the training process. The derived coefficients using the CFD training dataset are presented in Table 5-5.

Table 5-5: Correlation coefficients for H₂ micromix combustor

Coefficients	a	b	c	d
Value	0.0864	0.40	190.89	1.95

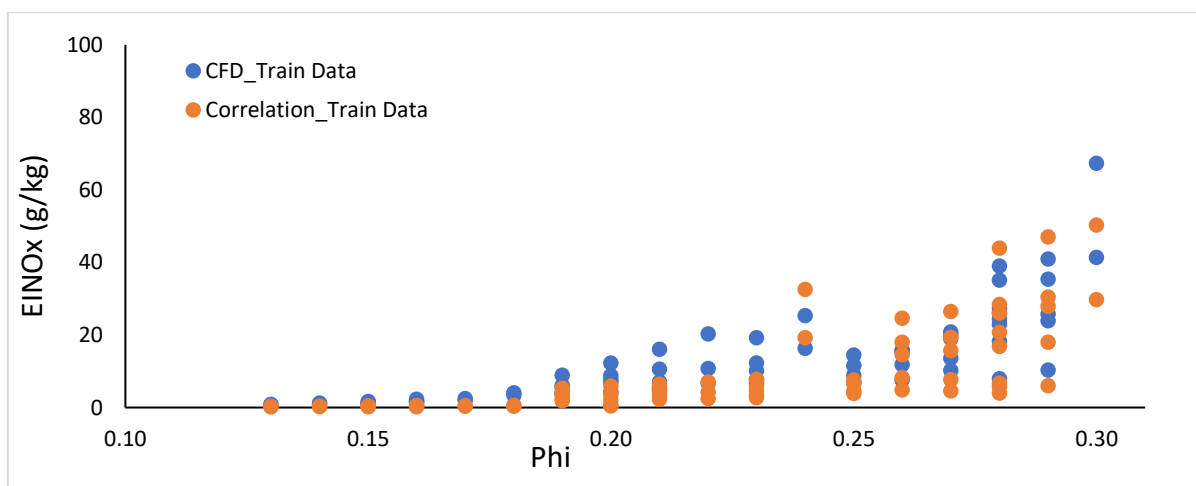


Figure 5-15: The EINOx correlation comparison against CFD data

5.9.3 H₂ Micromix EINO_x ISA-SLS Humidity Correction

The standard practice for deriving EINO_x correlation is from experimental data obtained at ISA-SLS conditions with a relative humidity (RH) of ~60%. The correlation and corresponding values of the coefficients presented in Section 5.9.2 were based on a dry air assumption. The humidity corrections applied to the correlation are presented below.

Figure 5-16 is a chart that is used for NO_x humidity correction. It illustrates the influence of RH and altitude on the NO_x emissions humidity correction factor (e^H). The correction applied to the correlation displayed in Equation 13 to account for ~60% RH at ISA-SLS is shown in Equation 14.

$$EINO_x = 0.0864 * \left(1 - (e_{RH0}^H - e_{RH60}^H)\right) * P_3^{0.40} * e^{\frac{T_3}{190.89}} * \phi^{1.95} \tag{Equation 14}$$

Where:

$H = -19(\omega - 0.006344)$ is the humidity correction factor

ω is the specific humidity at the required altitude

e_{RH0}^H is the value of e^H at relative humidity of 0% at SLS conditions (1.125)

e_{RH60}^H is the value of e^H at relative humidity of 60% at SLS conditions (1)

This results in the correlation shown in Equation 15

$$EINO_x = 0.0756 * P_3^{0.40} * e^{\frac{T_3}{190.89}} * \phi^{1.95} \tag{Equation 15}$$

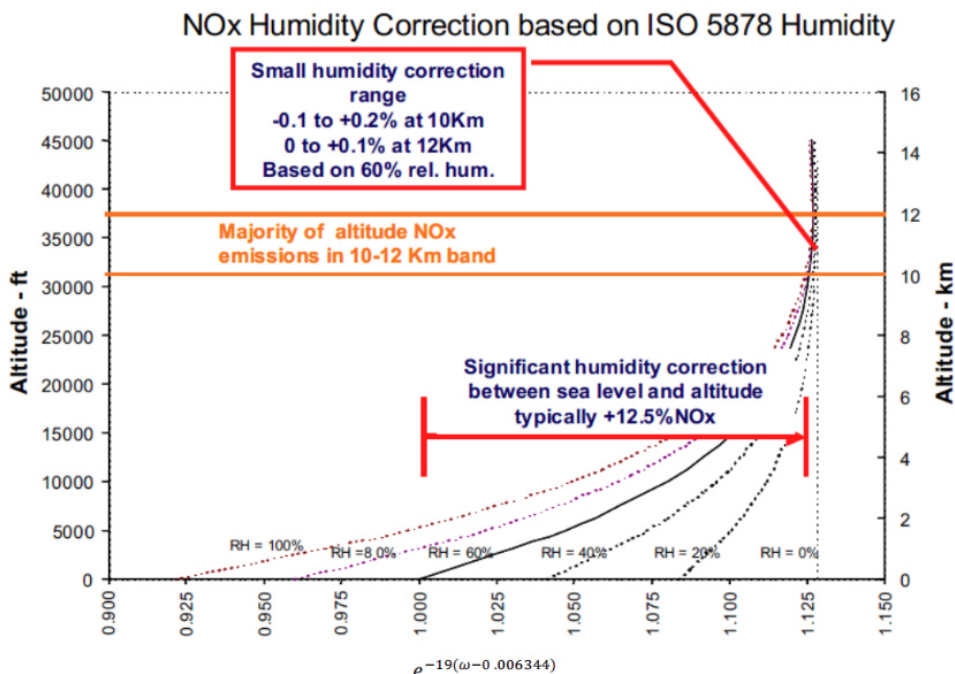


Figure 5-16: Humidity Correction factor e^H for NO_x at altitude [30]

5.9.4 Humidity Correction for Altitude

For the EINO_x correlation to be applicable for the entire flight envelope a further correction is required to account for the variation of humidity with altitude. This correction and the final proposed correlation (which accounts for the effects of altitude on relative humidity and consequently NO_x) is shown in Equation 16.

$$EINO_x = 0.0756 * P_3^{0.40} * e^{\frac{T_3}{190.89}} * \Phi^{1.95} * e_{Alt}^H \quad \text{Equation 16}$$

Where:

e_{Alt}^H is the value of e^H corresponding to altitude and the RH at that altitude. In the event that the RH is not known for given altitude it is recommended to use the e^H value corresponding to RH 60%.

Note, humidity corrections to EINO_x correlations are only necessary if:

- Engine performance is modelled assuming dry air, which tends to overestimate the highest engine gas temperatures at a thrust when compared to more accurate performance calculations taking humidity into account.
- CFD simulations used to derive the correlation assume dry air.

This correlation was used for the mission-level NO_x emissions predictions in ENABLEH2 WP1. The detailed analysis and results are reported in public deliverable D1.4 [2]. In summary, relative to the year-2050 Long-range Jet A-1 tube & wing design, NO_x is reduced by 39-43% by the LH₂ tube & wing aircraft and by 54-59% by the more efficient LH₂ BWB aircraft.

6 Thermoacoustic risk assessment and roadmap

6.1 Thermoacoustic Risk Assessment

6.1.1 Introduction

The introduction and development of new combustion technologies always carries the risk of suffering from damaging high amplitude thermoacoustic pressure oscillations. This was a particular problem when lean premixed combustion systems were introduced to replace diffusion flame combustors in land-based power generation gas turbines. Diffusion combustors have historically been less prone to thermoacoustic issues than lean premix combustion. The majority of aviation gas turbine combustors use diffusion-based (or partially premixed) combustion technologies, minimising the risk of issues with thermoacoustic instabilities and their consequent impact on combustor integrity and life.

Micromix is essentially a diffusion combustion technology, and it is tempting to assume that this will result in a low risk of thermoacoustic instabilities. However, conventional diffusion combustors have relatively long, diffuse, flames resulting in a spread of heat release over a significant proportion of the combustor length. This reduces the potential for acoustic coupling between the flame and characteristic acoustic modes of the system comprising the air and fuel supplies to the combustor and the combustor itself (subsequently referred to as the combustion system). Also, conventional diffusion combustors have many dilution and cooling holes in the combustor walls, and these add acoustic damping to the combustion system due to acoustic transmission out of the combustor and losses due to the interaction of the incoming air jets and the acoustic waves within the combustor.

However, even though the micromix concept is diffusion based the flames are very short with heat release concentrated in a small area. This tends to favour coupling between the flame and characteristic acoustic modes of the combustion system. Also, the micromix concept does not require additional dilution holes and cooling holes are kept to a minimum to maximise combustion air to generate lean combustion conditions for low NO_x. This will minimise the acoustic losses.

These features are very similar to those for lean premixed combustion and thus the potential for problematic thermoacoustic instabilities should be given serious consideration.

One significant difference between micromix and premixed natural gas or Jet A-1 combustion is the flame length and thus characteristic times for the flame. Lean premix flames have shorter more intense flames than conventional diffusion flames, and micromix flames are significantly shorter again. This may increase the intensity of coupling with combustion system modes if it occurs. However, for a given combustion system the lowest frequency that a flame will couple with is dependent on the reciprocal of the characteristic acoustic time for the flame (to allow phase matching). Thus, the lowest frequency at which thermoacoustically unstable modes occur will be higher for micromix flames than lean premix flames due to the shorter flames and shorter characteristic times. Natural acoustic damping in the combustion system tends to scale on wavelength and thus damping tends to be higher at higher frequencies, potentially offsetting the increase in intensity of the micromix flame.

This subjective assessment is consistent with the work of Ghirardo et al [31] who conclude that flames with long time delays are more likely to excite thermoacoustic instabilities in a given combustor than those with shorter delays. This is encouraging as the intrinsically short micromix flames have short delays.

6.1.2 Thermoacoustic Behaviour of a Hydrogen Micromix Aviation Gas Turbine Combustor Under Typical Flight Conditions

The thermoacoustic behaviour of micromix combustors for aviation has been assessed for two scenarios:

1. Replacement of a conventional Jet A-1 combustor with a micromix combustor within the pressure casing of an existing engine (i.e., as a potential retrofit (RF)).
2. Design of a new engine specifically for hydrogen micromix combustion.

6.1.2.1 Scenario 1: Replacement of conventional Jet A-1 combustor with a micromix combustor

Details of this study have been published [13] and the findings are summarised here.

This study developed a micromix combustor concept suitable to replace the Jet A-1 combustor in a modern three spool, high bypass ratio engine and derives the acoustic Flame Transfer Function (FTF) at typical engine operating conditions for top of climb (ToC), take-off, cruise, and end of runway (EoR). Values of key parameters were chosen based on data for the Rolls-Royce Trent 1000 [32] and a similar geometry was assumed as an example of its class.

The FTF was derived using CFD and FTF models based on a characteristic flame time delay. The relative thermoacoustic behaviour for the four conditions was assessed using the low order acoustic network code, OSCILOS.

A novel approach to the determination of the time delay from RANS CFD was used to enable the evaluation of the FTF. Considering the quasi-steady situation, the first volume expansion experienced by the incoming flow is when the temperature increases, either due directly to local heat release or due to mixing processes. When considering planar (mass weighted) temperature averages the rise from one plane to the next is representative of the progressive increase in volume experienced by the flow. The period over which the volume flow increases can be represented by the period over which there is a significant gradient of the temperature rise (see Figure 6-1), where the characteristic delay time for the flame, τ , is the mean value and the spread of delay times. In this case $\Delta\tau$ was also equal to the mean time. This is because the time at which temperature is seen to rise is zero and this represents the lower limit of the spread. It can be seen, Figure 6-1, that the form of the plot can be approximated by a “top-hat” distribution.

The time delay and spread of time delays calculated by this method for each of the four flight cases are given in Table 6-1.

Table 6-1: Time delays for micromix combustion cases considered

Condition	Mean delay, τ (ms)	Spread of delays, $\Delta\tau$ (ms)
Top of Climb	0.156	0.156
Take-off	0.142	0.142
Cruise	0.155	0.155
End of Runway	0.144	0.144

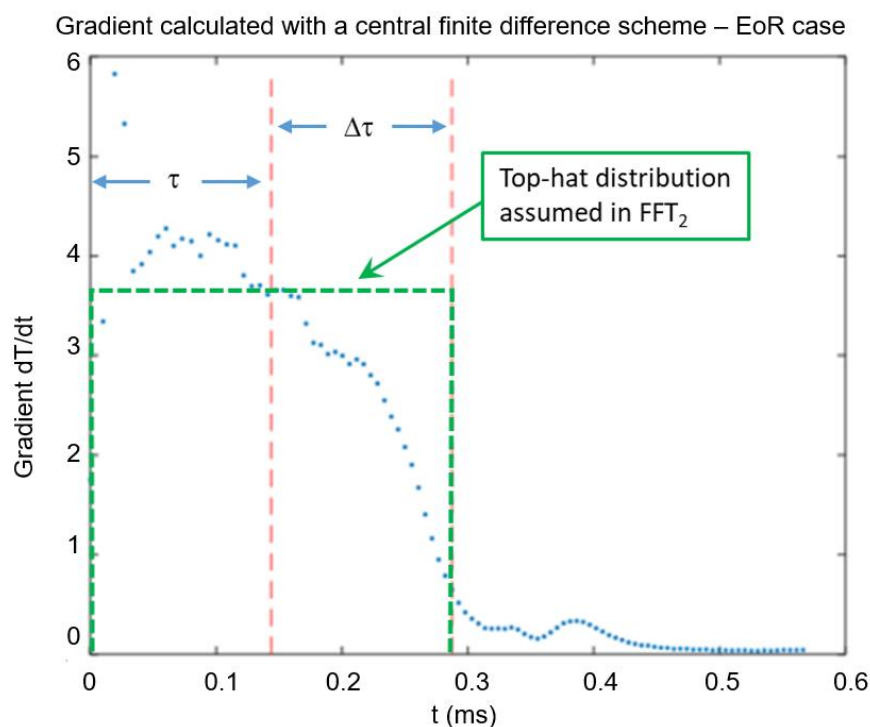


Figure 6-1: Example of the gradient of temperature rise calculated with a central finite difference scheme against mean propagation time along the combustor

Alternative formulations of the FTF using the time delays in Table 6-1 were considered:

The simple n - τ model is given by [33]:

$$FTF_1(\omega) = -ne^{-i\omega\tau} \quad \text{Equation 17}$$

where n is a constant representing the gain of the flame response and τ is a characteristic time delay for the flame.

This formulation does not account for the potential spread of time delays within the flame and tends to over-estimate the magnitude of the FTF, particularly at high frequencies.

A revised model proposed by Sattelmeyer and Eckstein, which assumes a “top hat” distribution of time delays, is given by [4]:

$$FTF_2(\omega) = -n\Theta e^{-i\omega\tau} \tag{Equation 18}$$

where Θ represents the effect of the spread of time delays and is given by:

$$\Theta = \frac{\sin(\omega\Delta\tau)}{(\omega\Delta\tau)} \tag{Equation 19}$$

and $\Delta\tau$ is the spread of time delays (i.e., the half width of the top hat distribution).

This formulation better represents the FTF at higher frequencies and was used for the analysis reported here.

Flame transfer functions calculated using FTF_2 for all four conditions are shown in Figure 6-2. It was observed that due to the very similar delay times, Top of Climb (ToC) and cruise are almost indistinguishable as are End of Runway (EoR) and Take-off.

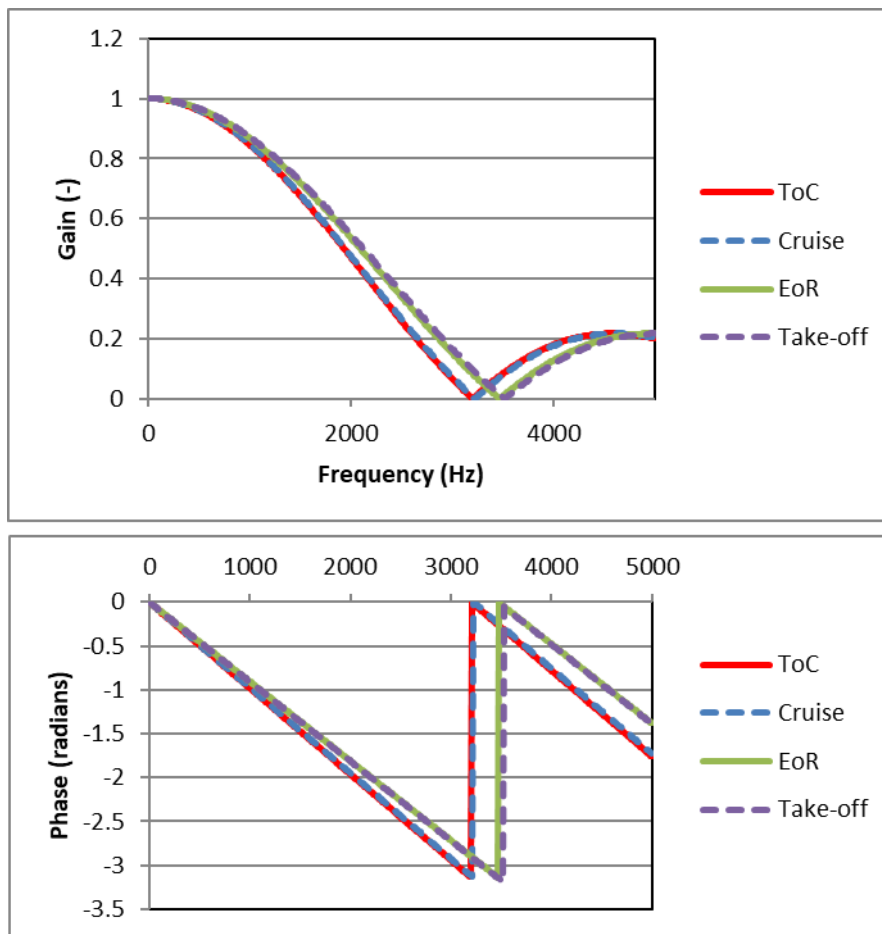


Figure 6-2: FTF calculated using FTF_2 and data in Table 6-1

These FTFs together with the geometry shown in Figure 6-3 were used to determine the frequency and growth rate of system longitudinal eigenmodes up to 4kHz for the four conditions, using the open source thermoacoustic code, OSCILOS-long developed by Prof. A Morgans and co-workers at Imperial College[34]. Eigenmodes predicted to have a positive growth rate represent frequencies at which high amplitude thermoacoustic oscillation can occur.

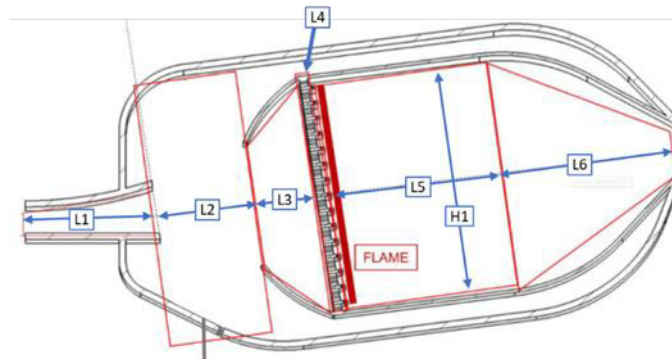


Figure 6-3: Combustor geometry used for the thermoacoustic assessments

Results shown in Figure 6-4 suggest that the risk of thermoacoustic instabilities associated with longitudinal waves at low frequencies (below 1kHz) is small, but that higher frequency longitudinal modes could be excited, with an unstable mode predicted at about 2kHz in all cases. The mode shape for the least stable modes (Figure 6-4) can be seen to be close to a half wavelength in the combustor.

Comparison with a Jet A-1 Lean Premixed Pre-vapourised (LPP) injection systems in the same combustor [13] showed that below 1kHz both combustors only had negative growth rate (i.e., stable) eigenmodes and that the micromix combustor had only a single eigenmode which had a lower growth rate (i.e. was more stable) than any of the four predicted modes for the LPP combustor. This suggest that at low frequencies the risk of thermoacoustic issues is lower than a Jet A-1 LPP combustor, which itself has low risk.

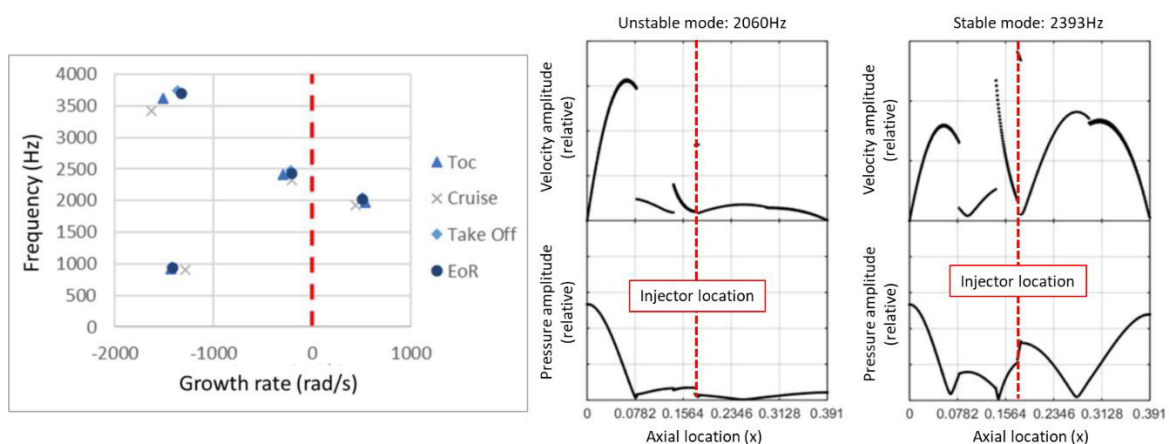


Figure 6-4: Comparison of eigenmodes for all micromix cases (left) and mode shapes for the two least stable modes for Take-off (centre and right)

The sensitivity of the combustor thermoacoustic behaviour to key combustor dimensions and characteristic time delay was also investigated [13]; this suggested that the predicted growth

rate of higher frequency longitudinal modes can be significantly influenced by combustion system design, giving potential for design changes to mitigate potential thermoacoustic issues. Also, the fact that the frequency of the predicted mode does not vary significantly with operating condition means that the use of tuned dampers such as Helmholtz resonators is likely to be an effective control measure across the whole operating range. Experience with land-based gas turbines has (e.g.[35]) has shown such resonators are effective and relatively small for high frequencies and can be effectively combined with cooling systems, thus reducing any weight penalty.

However, as the combustor is annular, circumferential and radial modes may also be excited and these were not considered in this analysis. Above the frequency for circumferential mode formation, circumferential, axial and mixed modes will be possible in the combustor. Above the frequency for radial (cross) modes, radial and further mixed modes will be possible. For the conditions considered, the frequencies of the first circumferential and radial modes are approximately 425Hz and 2700Hz respectively.

A version of OSCILOS (OSCILOS-ann) that can predict both longitudinal and circumferential modes in annular combustors is available, but it was not possible during this study to model the complex distributed nature of micromix combustion using this software.

However, the short time delays within the flame would still favour coupling with higher frequencies, thus only higher order circumferential modes would be expected with low order modes not being favoured. The fact that the predicted longitudinal modes are high frequency cannot be taken as direct evidence of the micromix flame only coupling with high frequency modes as the predicted mode shapes (Figure 6-4) of the two highest growth rate modes approximate to a half wavelength of the combustor. This is the first axial mode that would be expected to be excited. Thus, the high frequency of the first mode is associated with the short length of the combustor not specifically with the short time delay. However, predictions for micromix flames in a rig with a much longer combustor gave the first unstable mode to be three half wavelengths. Confirming that that short time delay micromix flames are unlikely to couple with low frequency system modes.

This, however, remains an area of significant risk as the potential for complex high frequency circumferential and radial modes has not been fully investigated. Limited information on micromix in small land-based gas turbines [36] has shown that high frequency (2 to 5kHz) travelling circumferential modes can occur in a cylindrical can combustor fired by micromix injectors. Each of the small micromix flames can behave differently from their neighbours depending on the local acoustic conditions and this could allow more complex modes to be generated than occur in a more conventional configuration with a relatively small number of burners/injectors.

It is encouraging that this simple approach used in a preliminary design suggests that:

- the micromix combustor has lower risk at low frequencies than a Jet A-1 combustor
- the risk of higher frequency modes can be reduced by appropriate combustion system design
- acoustic treatments such as Helmholtz resonators should be an effective control strategy for high frequency modes if required

However, more detailed thermoacoustic analysis together with experimental validation are required as the combustor design progresses to ensure that the risk of problematic thermoacoustic oscillations is minimised.

6.1.2.2 Scenario 2: Design of a new engine specifically for hydrogen micromix combustion

The preliminary design of a micromix combustor has been performed for a high bypass ratio turbofan engine for the ENABLEH2 Year 2050 long range, blended wing body aircraft (LR BWB 2050).

Figure 6-5 shows the combustor geometry. In OSCILOS-long the geometry is represented as a series of cylindrical sections each having the same length and cross section as the annular sections in the defined geometry. This results in the simplified geometry also shown in Figure 6-5.

Predictions for Scenario 1 indicated that there was relatively little difference in thermoacoustic behaviour for the different operating cases and analysis of Scenario 2 has been limited to two representative condition, Cruise and Top of Climb (ToC)

The FTFs for both conditions were determined from RANS CFD using the same methodology as Scenario 1 (see Section 6.1.2.1) and the resultant rise temperature rise gradient for the Cruise case is shown in Figure 6-6.

Results of τ and $\Delta\tau$ for both cases are given in Table 6-2.

Table 6-2: Results τ and $\Delta\tau$ for Scenario 2 combustor at Cruise and Top of Climb

	τ (ms)	$\Delta\tau$ (ms)
Cruise	0.139	0.149
Top of Climb	0.055	0.080

It can be seen that τ and $\Delta\tau$ are much shorter than those calculated in Scenario 1 (Table 6-1). This is due to a significantly different injector design being used in this combustor, which has been chosen to reduce NO_x production and has a much more compact flame.

This results in significantly different FTFs to Scenario 1 (Figure 6-7). This together with the modified geometry results in higher predicted eigen mode frequencies in Scenario 2 (Figure 6-8).

However, the mode shapes of the two most unstable modes (Figure 6-9) are very similar within the combustor to those predicted for Scenario 1 (Figure 6-4) and are approximately a half wavelength, but the mode shapes upstream of the combustor are quite different, emphasising the influence of combustor geometry on mode frequency.

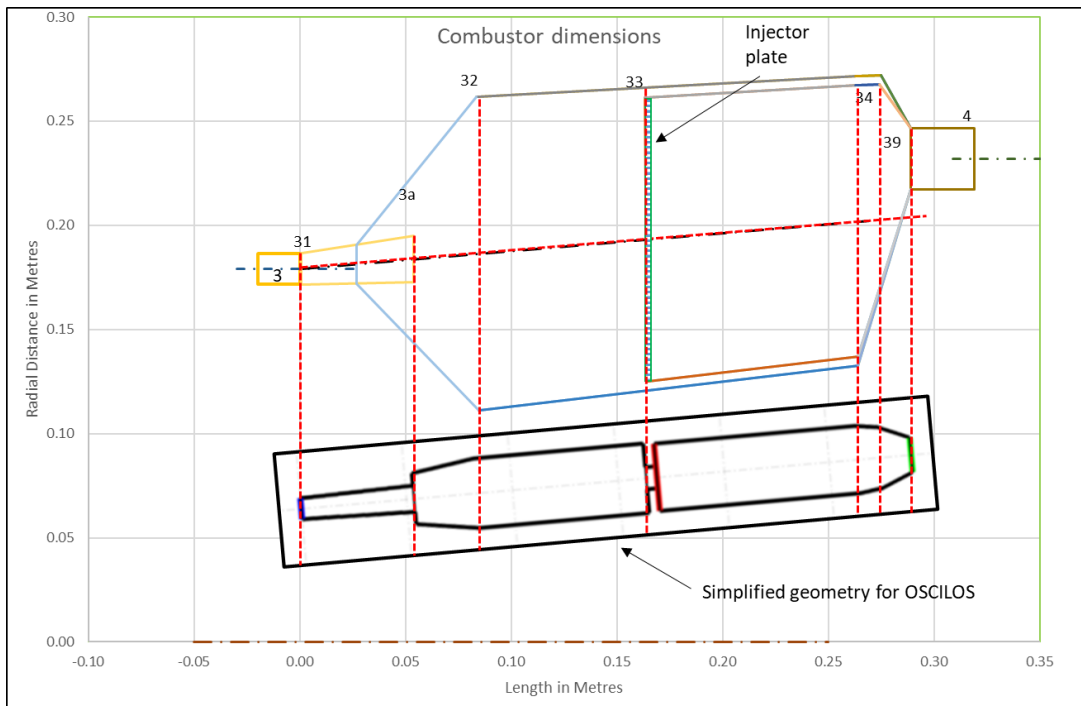


Figure 6-5: ENABLEH2 combustor design compared with simplified geometry used for the thermoacoustic analysis in OSCIOS

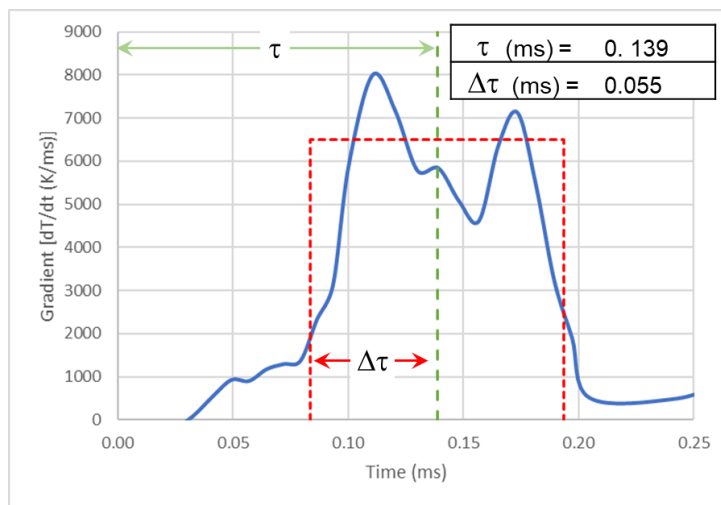


Figure 6-6: Gradient for cruise conditions showing “top-hat” approximation to temperature rise distribution

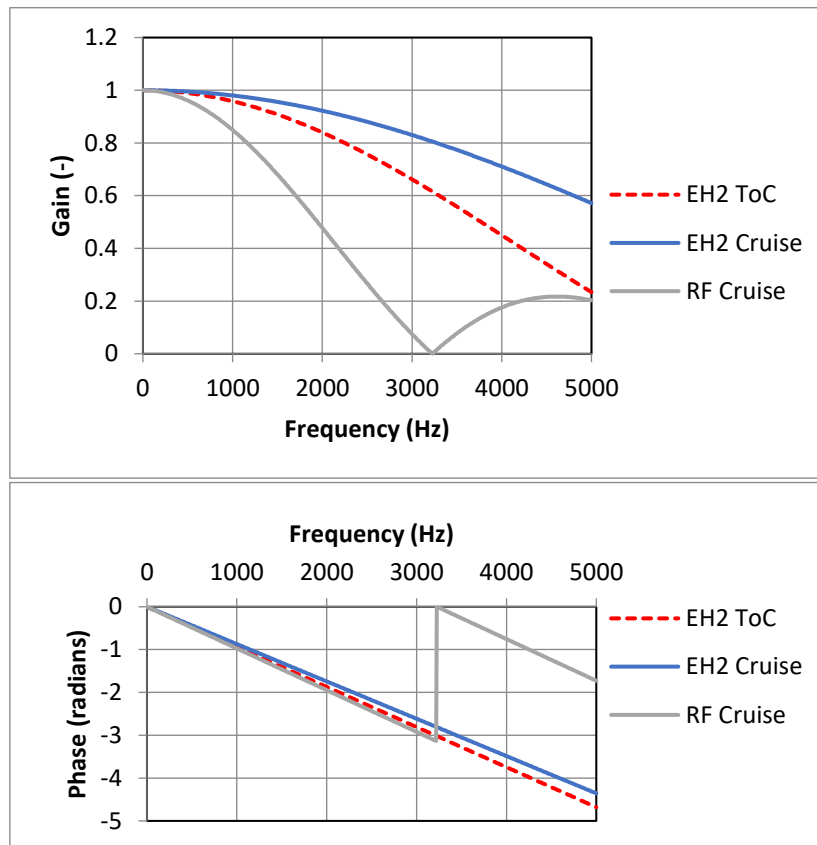


Figure 6-7: FTFs for Scenario 2 (ENABLEH2 “EH2”) combustor for Cruise and ToC. Scenario 1 (Retrofit “RF”) FTF included for comparison

As with Scenario 1, circumferential and radial modes need further investigation, however the similarity of the behaviour of these two significantly different geometries and flame responses supports the findings of Section 6.1.2.1

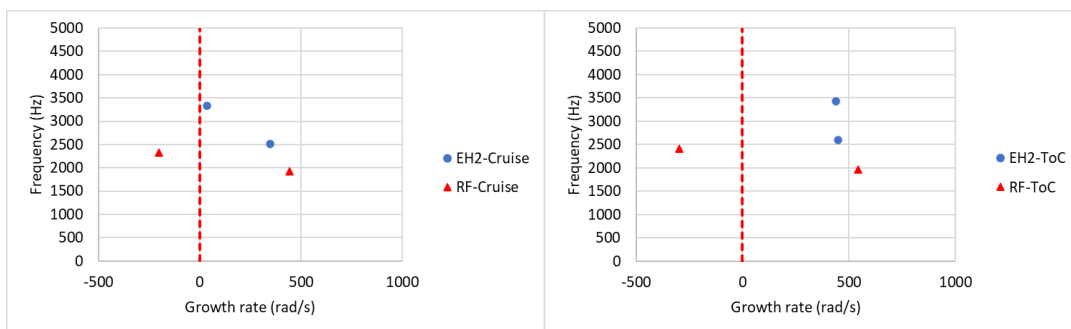


Figure 6-8: Comparison of eigenmodes for Scenario 1 (ENABLEH2 “EH2”) and Scenario 2 (Retrofit “RF”) for Cruise (left) and ToC (right)

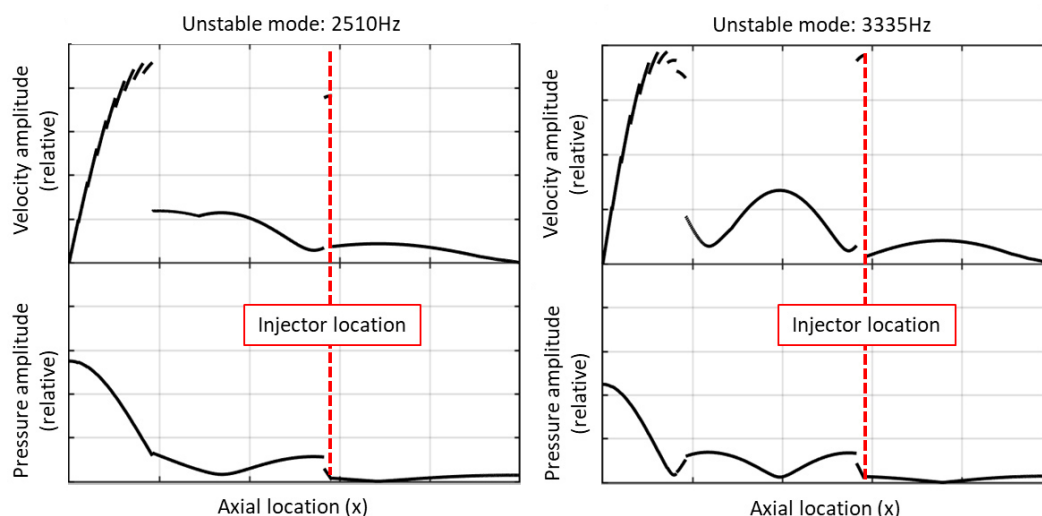


Figure 6-9: Mode shapes for the two most unstable modes for Cruise conditions (Scenario 2)

6.1.3 Other periodic instabilities

In addition to the thermoacoustic instabilities assessed in Section 6.1.2, other potential instabilities have been identified. LES models of a small numbers of micromix injectors configured to simulate an infinite array of injectors showed unexpected high frequency pressure oscillations. This was investigated with further LES modelling and is reported in Sun et al. [37]. Figure 6-10 shows key results of this investigation. A strong peak is seen in the pressure amplitude at the air gate with a frequency of 23.8kHz (left hand image). The right-hand image shows the progress (top to bottom) through a period of oscillation. Column (a) shows pressure contours and it can be seen that highest pressures (red and blue) occur within the air gate and that the pressures downstream of the air gate are low (green).

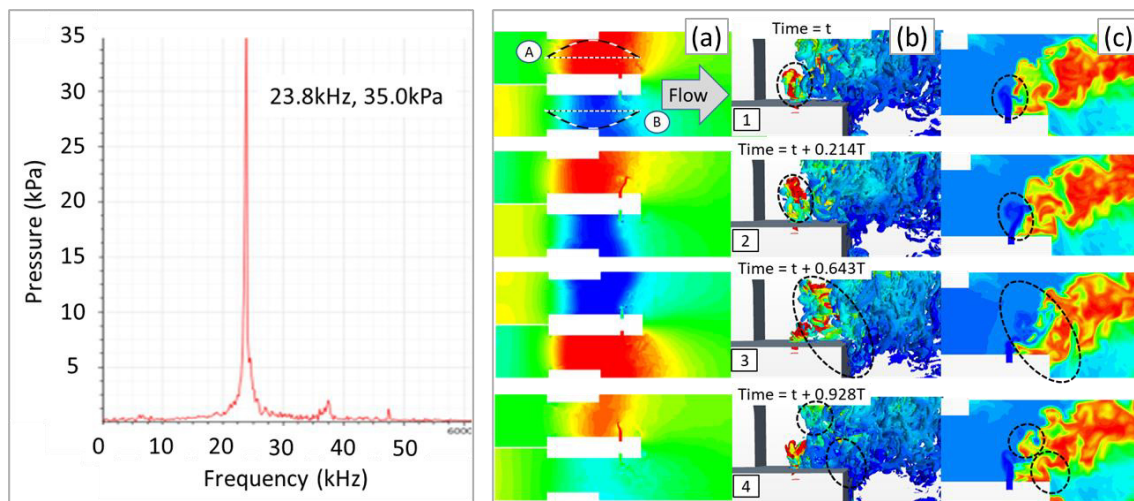


Figure 6-10: Left-hand image: Pressure spectrum observed in an LES model of a baseline micromix injector array. Right-hand image: Stepping from top to bottom through an instability cycle of period T . [(a) pressure contours in a pair of injectors. (b) flow structure in upper injector. (c) temperature contours in upper injector]

The investigation concluded that it was likely that the instability was linked to feedback from the trailing edge of the injector plate to the fuel injection port involving sub-harmonic interaction

with the upstream formation of ring vortices. Figure 6-10 right, columns (b) and (c) show the formation of a vortex generated by the agglomeration of several ring vortices (circled in rows 1 and 2). This leads to the formation of opposing large vortex pairs (circled in rows 3 and 4). It is likely that this was significantly enhanced by a half wave resonance along the length of the injector plate (Figure 6-10 right column(a)). Thus, to reduce the risk of such instabilities in practical injectors the design of the injector should consider the relationship between the convection time (related to the phase speed of convective disturbances) from the fuel nozzle to the trailing edge of the injector plate and the period of a $\frac{1}{2}$ -wave acoustic mode along the injector plate. Attention should also be paid to the dynamic characteristics of the fuel jet, such as the formation of ring vortices, and the possibility of sub-harmonic interactions. Such oscillations have not yet been reporting experimentally and were not detected during combustion testing as part of the project but remain a potential (theoretical) risk.

The possibility of self-excitation by aerodynamic effects such as vortex shedding exists in any flow system and LES modelling of combustion rig tests of a micromix injector identified such instabilities[38]. Figure 6-11 shows the predicted spectra of air gate velocity and combustor OH mass fraction seen in the LES model. A strong characteristic peak at 2450Hz is seen in both spectra suggesting an aerodynamic instability that could couple with flame acoustics.

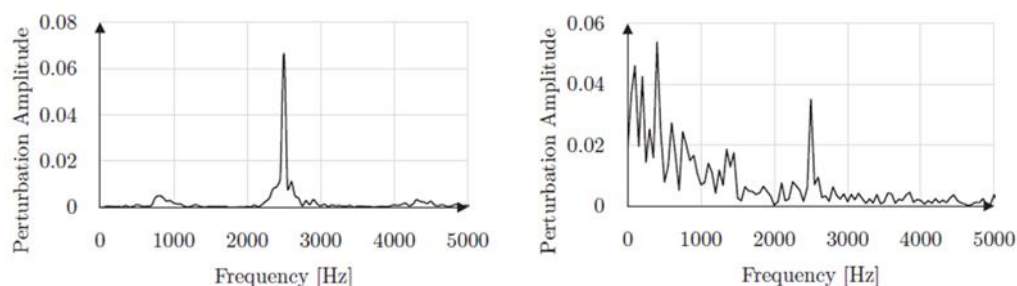


Figure 6-11 Spectra of the velocity at the air gate (left) and the mass fraction of OH in the combustion zone (right) (from [38])

It was concluded that this was an aerodynamic instability associated with vortex generation at the injector plate. Acoustic data from combustion tests showed no evidence of such instabilities, however consideration of the potential for coupling between aerodynamic instabilities and flame acoustics should always be considered during combustion system design.

6.2 Risk Summary

6.2.1 Hazards Identification.

The introduction and development of new combustion technologies always carries the risk of suffering from high amplitude thermoacoustic pressure oscillations. This potentially generates the following unwanted consequences and hazards:

1. Damage to combustor components due to vibration induced high cycle fatigue, potentially leading to:
 - Reduced component life
 - Combustor failure leading to engine failure
 - Consequential damage (thermal or domestic object damage) to other engine components
2. Vibration induced wear of components leading to:
 - Reduced component life
 - Increased leakage at component interfaces affecting, efficiency, emissions, combustion dynamics and operability
3. Increased heat transfer to combustor components leading to:
 - Reduced component life
 - Combustor failure leading to engine failure
 - Consequential damage (thermal or domestic object damage) to other engine components
4. High acoustic velocity amplitudes leading to:
 - Acoustically induced flashback causing component damage and consequences as (1) above
 - Acoustically induced flame blow-off leading to flame failure

Thus, it is essential that thermoacoustic instabilities are ideally prevented but as a minimum, amplitudes must be limited to non-damaging levels.

6.2.2 Risks Assessment

High amplitude pressure oscillations in combustors systems can be produced in three main ways. An additional mechanism generating high amplitude oscillations within a micromix injector is also considered:

1. Forced oscillations:

Flames act as acoustic velocity amplifiers and also produce acoustic output due to factors such as oscillatory fuel concentration entering the flame. Such oscillatory inputs to the flame will be amplified and could produce high amplitude acoustic velocity and pressure waves in the combustor. These oscillatory inputs can come from aerodynamic effects in the air or fuel supplies or factors such as oscillatory fuel injection due to fuel valve control instabilities.

Factors such as fuel valve control instabilities should not be a problem in a well-designed system and if they do occur can be corrected without recourse to expensive combustion system redesign.

Aerodynamic instabilities (such as vortex shedding) generating oscillatory air or fuel inputs to the burner/flame region should be avoided by careful aerodynamic design. If they do occur, they do not usually result in damaging combustor pressure amplitudes unless they couple with thermoacoustic feedback instabilities (see below).

Thus, unless coupling with acoustic feedback occurs, forced oscillations can be regarded as low risk and their avoidance is a normal part of good design and development.

2. Aerodynamic and coupled instabilities:

Aerodynamic features of the burner/injector and flame zone (e.g., vortex shedding and shear layer instabilities) can directly produce oscillatory heat release and generate pressure oscillations in the combustor. The velocity and OH (thus heat release) seen in the LES model of a micromix test rig injector (Figure 6-11) are an example of this.

Such instabilities may affect the flame's acoustic response (as represented by its flame transfer function) and couple with acoustic feedback instabilities (see below), increasing the incidence of thermoacoustic feedback and possibly increasing its severity.

3. Acoustic Feedback:

This is usually the most significant cause of unacceptably high amplitude pressure oscillations in high intensity combustion systems such as gas turbine combustors and occur due to the feedback represented in Figure 6-12. This results in growing fluctuations when the fed back signal is in phase with the original disturbance and the losses in the loop are less than the gains.

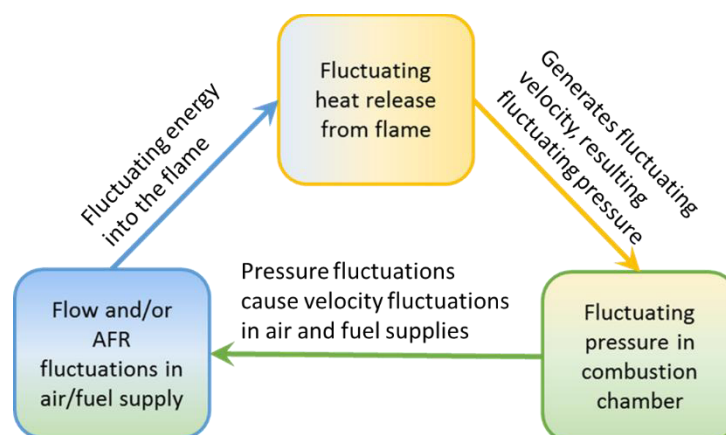


Figure 6-12: Thermoacoustic feedback loop

Such feedback oscillations are a function of the interaction of the acoustics of all parts of the combustion system with the flame and are typically difficult to eliminate without significant changes to the combustion system or flame behaviour (e.g. by burner/injector redesign) and it is important to be aware of this throughout the combustor design to prevent the need for costly re-design or treatment late in the development process.

The potential for such feedback oscillations in hydrogen micromix fired aviation gas turbine combustors were assessed and have been presented in Section 6.1.2.1 (for a retrofit to an

existing engine) and Section 6.1.2.2 (for a new aviation gas turbine). This assessment showed that the risk of low frequency instabilities (below 1kHz) is low, but that there is a risk of higher frequency unstable modes. The risk may be lower than indicated by the growth rates predicted in this analysis as the impact of acoustic losses including those due to cooling arrangements were not included in this early analysis as the preliminary design did not include sufficient details of cooling arrangement to include in the thermoacoustic model. Thus, losses are underestimated, and growth rate will be over-estimated. Also, such losses tend to increase with increasing frequency and are likely to be significant at these high frequencies. However, the risk of thermoacoustic feedback oscillations must be taken seriously. Also, the analyses presented in Sections 6.1.2.1 and 6.1.2.2 do not directly consider circumferential modes, but postulate that only high frequency circumferential modes will be excited due to the short characteristic flame times that will occur in such flames. The behaviour of circumferential and radial modes remains the most significant unknown with the following open questions:

- Can low frequency circumferential modes be excited despite the short flame characteristic times?
- Does the distributed nature of the micromix injector allow more complex circumferential, radial and mixed modes to generated?

4. Injector instabilities

The generation of high amplitude pressure oscillations within a micromix injector has been observed in LES simulations of an injector plate (Section 6.1.3). This was linked to the interaction between aerodynamic instabilities in the fuel jet and the acoustics of the injector plate. This phenomenon has not been observed experimentally but should not be ignored.

6.2.3 Control and mitigation of the risks.

The risks should be considered throughout the design process as indicated in the Design and Development Roadmap (Section 6.2).

Forced oscillations are low risk and should be avoided by normal good design and development.

The occurrence of aerodynamic instabilities which can couple with thermoacoustic instabilities should be assessed and potential interaction avoided by modified design.

Thermoacoustic analysis should be performed to understand likely unstable modes. If unacceptable unstable modes are predicted the risk of such modes can be reduced by the following means:

1. Modification of the flame acoustics:

This could be achieved by changing the injector design; however, this may adversely impact other combustion performance parameters.

The use of injector fuel staging can be used to modify the overall flame acoustics. Fuel staging is where with an array of identical injectors, some groups are fired at above and others below the design equivalence ratio but with the average meeting the design requirement. This results in the flames in the zones having different characteristic times and thus different acoustic properties. The arrangement of zones and their deviation from the design value can be varied to give maximum acoustic benefit. However, this will have some impact on other combustion parameters such as emissions and this needs to be taken into account.

Fuel staging can be achieved either by having groups of injectors fed from separately controlled fuel delivery systems allowing the fuel to different groups to be controlled separately. This gives most flexibility of control, but adds complexity, some weight and cost. Alternatively fixed orifices can be used to change the proportions of fuel to different groups of injectors. This gives less control flexibility but may be an acceptable approach.

Alternatively, injector staging may be used. This is where the design of some groups of injectors are modified to have different properties. The simplest method of injector staging is to modify the air gate to produce a different air flow in different groups injector while the fuel flow is kept the same in all injectors. This results in different equivalence ratios in the different groups of injectors in a similar way to fuel staging with fixed orifices.

If controlled fuel staging were implemented, it would be possible to use “Reactive Control” where the control system detects the onset of instabilities and changes the fuel split to the staging arrangement to compensate and suppress oscillations. This is now widely implemented in land-based gas turbines in the form of autotuning systems [39] and has potential for aviation applications.

2. Modification of combustion system acoustics:

This can be achieved by changes in the overall combustion system design. If issues are identified early enough in the design process it may be practicable to modify the combustor geometry to reduce the risk of problematic thermoacoustic oscillation. Analysis has shown (Section 6.1.2.1 and Ref.[13]) there is significant potential for geometry changes to reduce the risk of thermoacoustic issues. However, considerations of compatibility with the engine architecture and combustion performance requirements may limit the possible changes.

The system acoustics may be modified by added features such as perforated plate dampers or tuned resonators.

Perforated liners with air flow through them act as acoustic dampers, cooling and dilution holes in the combustor may add damping in the same way as perforated liners, but are not acoustically optimised. These are likely to be fewer in micromix combustors than in conventional aviation combustors. Damping depends on pressure drop and flow through the perforated plate and this can be adjusted by use of double screens. A comprehensive review of the theory of perforated liners is given in Lahiri and Bake[40].

Helmholtz resonators are the tuned damping devices most commonly used in land based gas turbine combustors and modify the acoustic behaviour of the system at particular frequencies which can be matched to known thermoacoustic frequencies. These resonators may be added to the burner, combustor, air supply or fuel supply, but typically they are added to burner or combustor. Multiple resonators may be used for increased effect and/or increased frequency coverage and multi-volume interconnected resonators can have a wider frequency range [41] allowing for changing instability mode frequency as operating conditions change.

It is possible to consider the combination of cooling arrangements and perforated plate dampers and Helmholtz resonators to optimise overall performance. One practical application of this is the incorporation of multiple interconnected Helmholtz resonators into the combustor cooling system of a power generation gas turbine to suppress high frequency instabilities as reported by Schuermans et. Al [12]

Addition of such control devices will add weight and cost to the system but have little or no impact on combustion performance (e.g., emissions) unlike measures such as staging. Such

treatments tend to be more effective and are smaller and lower weight when applied to higher frequency modes. The analysis to date suggests that only high frequency modes are likely to be of concern, thus such treatments are likely to be effective if needed.

3. Active Control:

Active control of thermoacoustic instabilities has been successfully applied to land based gas turbines by Siemens (Hermann et al.[42]). In this implementation an actuator modulates part of the fuel flow to produce pressure fluctuation (via heat release) in anti-phase to the acoustic oscillations, thus in principle suppressing the instability. This was found to be effective in suppressing unwanted instabilities in practice. Active control is often less robust than passive measures and Siemens no longer apply it to new machines, however, active control for thermoacoustic instabilities is commercially available (e.g. Ref. [43]). These applications are typically of the order of 100-300Hz, and it would be more difficult to implement at the high frequencies anticipated in micromix aviation combustors due to the high speed of response needed for the control valve modulating the fuel flow.

6.3 Micromix Combustor Thermoacoustic Design and Development Roadmap

Thermoacoustic design has to be an integral part of the overall combustor design process because late identification can lead to costly re-design late in the development process. Figure 6-13 show an overview of the preliminary design process and similar interactions continue through the combustor development and detailed design phase. Thermoacoustics are as important a consideration as heat transfer and cooling through its impact on combustor life and integrity and like emissions contributes to the overall environmental impact of the engine through its impact on engine noise.

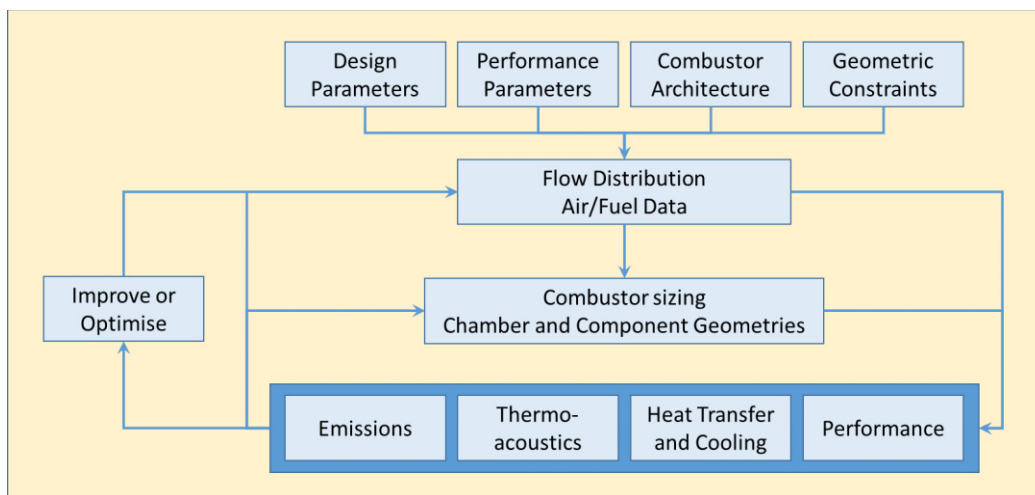


Figure 6-13 Global design framework for preliminary combustor design (modified from [10])

Thermoacoustic analysis can be carried out at various levels of fidelity, and this should be matched to the status of the design and the level of detail and resources available.

Detail available at the preliminary design stage is suitable for analysis using Network codes together with estimates of the FTF based on characteristic delay times determined using RANS CFD together with an analytical model (see Section 6.1.2.1 and [13]) or directly from LES CFD (see [37] and [44]). If the injector design is particularly well developed, experimentally determined FTFs may be available, and these should be used where possible.

Most manufacturers have their own in-house thermoacoustic network codes as do a number of universities. These are in principle capable of analysing all types of mode in the combustor and are a useful tool. For organisations that do not have in-house codes, a family of open source thermoacoustic network code (OSCILOS) is freely available [34]. However, the distributed nature of the micromix injection system makes it difficult to model circumferential and radial modes using network codes and this is an area requiring further development.

Numerical modelling of gas turbine combustion (both RANS and LES) is a well-established part of the design process, but models for Jet A-1 combustion (for aviation gas turbines) and natural gas combustion (for aviation gas turbines) have been developed and improved over several decades and a large body of experimental data for model validation exists. This is not the case for combustion of hydrogen in gas turbines and more development in this area and the production of experimental validation data will improve the accuracy of these models and reduce the risk of unexpected issues late in the design process.

During the detailed design phase, more precise network modelling, ideally using measured FTFs, may be used to optimise the geometry and model the effects of treatments such as Helmholtz resonators and perforated plate dampers if required to ensure adequate provision of space and mass for such treatments. It may also be appropriate, if sufficient computing resources are available, to confirm the combustion behaviour, including thermoacoustics with detailed LES simulations as described in Wolf et al [45] and Poinso [46].

Direct experimental simulation/determination of on-engine thermoacoustic behaviour is difficult unless performed in a full engine environment at representative conditions because the full engine configuration from compressor discharge to turbine inlet has a profound effect on the thermoacoustic response of the combustion system. The acoustic boundary conditions represented by the last stage of the compressor (upstream) and first stage of the turbine (downstream) are difficult to simulate during rig tests. It is more appropriate to use rig tests, including full annular tests to validate and refine network modelling procedures by modelling the rig tests, including appropriate boundary conditions. These can then be applied with greater confidence to full on-engine simulations.

Applying these procedures throughout the design process will minimise the risk of unexpected problematic thermoacoustic instabilities, but as with all combustion processes final on-engine tests at representative conditions are needed to confirm thermoacoustic behaviour.

The following enablers would facilitate this design and development process:

1. Development of CFD methods for hydrogen combustion

Improvement of CFD methods for hydrogen combustion and the generation of appropriate experimental data for model/method validation would benefit all aspects of combustion design including thermoacoustics. Further development of methods of determining Flame Transfer Functions (FTFs) will enhance network modelling capabilities.

Access to very high-performance computing facilities would facilitate the development of LES models of complex geometries allowing thermoacoustic behaviour to be directly modelled without recourse to thermoacoustic network codes.

2. Development of low order thermoacoustic codes

Network models (or other low order codes such as Helmholtz solvers) need to be able to deal with the full range of possible modes i.e., axial, circumferential, radial and mixed modes in annular combustors. The difficulty of modelling the distributed nature of micromix injectors needs to be addressed to fully represent annular combustors. Modelling of fuel staging needs to be developed to allow this control strategy to be evaluated and improved.

3. Development of passive acoustic dampers

The development of passive acoustic damping technologies to mitigate thermoacoustic risk will enhance control options. Existing technologies such as perforated plates and Helmholtz resonators can be improved, and novel treatments should also be considered. The development of any damping technology must consider space and weight requirements and the combination of acoustic damping and combustor cooling may be a fruitful area of research.

4. Rig testing capability for FTF determination

Limited facilities exist for the determination of FTFs under representative conditions. Development of such facilities and the development of methods of scaling FTFs from low

pressure measurements to engine-representative conditions would enhance the development process.

5. Reactive control of staging and alternative control strategies

Fixed staging and controlled staging add relatively little weight to the engine and may be preferable to the use of passive acoustic dampers which can take significant space and add weight. However, staging will tend to increase NO_x emissions. Reactive control of staging (i.e., the control of staging in response to detected combustor conditions) is a potential strategy with low impact on the engine architecture and may be used to minimise the impact of staging on NO_x. Development of staging control strategies will significantly enhance acoustic control options.

Experience of land-based gas turbines, together with the predicted high frequency nature of potential issues with micromix thermoacoustic, suggest that reactive control of staging (auto-tuning) will prove more fruitful than active instability control, but research into active control technologies should still be further researched.

7 Conclusions and Recommendation

The following key technical outcomes were achieved in ENABLEH2 WP3.

- Best practices for hydrogen micromix combustion numerical modelling were established by:
 - Comparing different turbulent-chemistry interaction models
 - Investigating the effect of several multi-component diffusion models on flame and temperature characteristics
 - Calibrating RANS model constants with LES
- The impact of key design parameters on flame temperature, residence time, recirculation zone position, flame-flame interaction and NO_x generation were assessed via design space explorations.
- The performance and NO_x emissions of three different micromix injector prototypes in a high-pressure high-temperature combustion rig was investigated for air inlet pressures up to 10bar, temperatures up to 585K, and equivalence ratios ranging from 0.3 to 0.5.
- An injector design that has the potential to deliver ultra-Low NO_x emissions without compromising the other performance and operability criteria was identified.
- The ignition performance at high altitude conditions was simulated at various conditions using YALES2 and AVBP. For ease of ignition, it is recommended to position the ignitor immediately downstream of injector and increase jet penetration via a stoichiometric equivalence ratio.
- A hybrid manufacturing approach has been proposed for the intricate designs of low-NO_x H₂ micromix injectors namely:
 - Additive Manufacturing of the injector plate with sophisticated internal hydrogen fuel manifold (to minimise the risk of hydrogen leakage)
 - Conventional Micro EDM for sub-millimetre circular orifice drilling for precision
- Methodologies were developed for:
 - Preliminary aerodynamic sizing and general arrangement of a hydrogen micromix combustor for a high bypass ratio turbofan engine for a Year 2050 long range, blended wing body aircraft (LR BWB 2050). Using the injector geometry down-selected from the numerical and experimental studies, it is expected that the combustor will require ~11000 injectors with an energy density of 6.7MW/(bar·m²).
 - Air and fuel staging for pilot and main injectors for a typical aircraft mission profile. Through fuel staging, the momentum flux ratio and equivalence ratio of individual injector can be maintained close to desired values for low emissions.
- A reduced order NO_x emissions prediction correlation was derived from higher-fidelity CFD simulations, for mission-level assessments and optimization.

- The risk of combustion instabilities for hydrogen micromix combustor for aero engines was assessed. It was concluded that:
 - There is lower risk of lower frequency instabilities relative to a Jet A-1-fuelled combustor.
 - The risk of higher frequency instabilities can be reduced by appropriate combustion system design and fuel staging.

Other key conclusions and recommendations from the study are as follows:

- As mentioned in Section 3.3.4, for a fair comparison of different fuels, an energy-based metric (g of emissions / MJ of fuel) should be used instead of the standard mass-based emissions index (EINO_x). It is recommended that EEINO_x, defined below is used to provide a fairer basis of comparison.

$$EEINO_x = \frac{EINO_x}{LHV}$$

- A relatively low momentum flux ratio injector design has the potential to achieve lowest NO_x, and NO_x has shown to notably increase for equivalence ratio above 0.4. Overall, the measured NO_x is more than 50% lower than a state-of-the-art Jet A-1 combustor at similar conditions.
- Relative to the year-2050 Long-range Jet A-1 tube & wing design, NO_x is reduced by 39-43% by the LH₂ tube & wing aircraft and by 54-59% by the more efficient LH₂ BWB aircraft.
- For combustion modelling, LES should be adopted wherever affordable. RANS are generally overly sensitive to the turbulence-chemistry interaction, which are governed by both the models and constants used. Flame length and temperature could vary significantly. With LES, this uncertainty is significantly reduced. Multi-component diffusion with a complex chemistry model should be used with LES to capture the impact of differential diffusion, which more accurately predicts a (higher) flame temperature than simpler chemistry models (that are less computationally expensive).
- Reaction zone imaging reveals important information about flame structures and mixing quality and provides an insight on the underlying phenomena. This is critical for comparing experimental and CFD-predicted flames, allowing for the calibration of the numerical models. However, recurring devitrification significantly limited the amount of flame imaging data gathered during the experimental campaign. For further research beyond ENABLEH2, an improved window design, with an active cooling configuration is suggested, to enable high-quality flame imaging data being obtained.
- As shown in Figure 4-6, the prediction of the precise location of the “transition points” A and B are critical in determining the ideal low NO_x design. Using the good modelling practices described above, effort should be made to calibrate flame positions against flame imaging data so that the impact of small variations of momentum flux ratio on NO_x can be better captured by CFD tools.

- Within a micromix combustor, the distribution of static pressure upstream of the injector plate is critical to ensure uniform distribution of air mass flow rate towards each air gate. Therefore, dedicated effort should be made in designing a flow rectification device with acceptable pressure loss and length. This could be highly challenging due to the distortion of the flow caused by the dump diffuser upstream.
- More cost-effective hydrogen micromix injector manufacturing approaches are required. The hybrid approach proposed above is both expensive and time-consuming. More advanced AM techniques should be developed so that the micromix injection system can be manufactured as one piece in its entirety.
- Material performance characteristics for H₂ fuel systems should be further investigated (e.g. deterioration, embrittlement, leakage etc.) as well as injector surface cooling due to the relatively “short” H₂ flames.
- Due to the constraints and challenges associated with SOA manufacturing techniques, as well as operation and maintenance, it is worth investigating the scalability of micromix injectors to reduce the total number of injectors. The size of injector should only be increased without significantly compromising NO_x emissions. Such modifications have already been tested for industrial gas turbine application. This will be more challenging for aero engine applications due to higher operating conditions. However as discussed in the ENABLEH2 Roadmapping Report (public Deliverable D5.2 [47]), for the first generation of hydrogen engines, one should focus more on delivering a fully operational hydrogen combustion system that is not necessarily optimised for low NO_x. Subsequent designs may then focus on design optimisation for ultra-low NO_x.
- It is also important to assess integration of the combustion system in the engine with respect to the fuel supply, control system and installation including the accessibility and ease of maintenance as well as aircraft system integration.
- To identify H₂ engine cycles that will deliver minimum environmental impact, it is recommended that Technoeconomic Environmental Risk Assessment (TERA) studies (design space exploration and MDO / trade-off studies) are performed to assess the implications of engine cycle parameters on mission fuel burn, NO_x and Contrails.

References

- [1] Airbus Deutschland GmbH, "Liquid Hydrogen Fuelled Aircraft - System Analysis," *Cryoplane*, no. May 2003, pp. 1–80, 2003.
- [2] A. Rolt, D. Nalianda, P. Rompokos, and I. Williamson, "Technology and scenario evaluation studies and benchmarking, ENABLEH2 Deliverable Report," 2023. doi: <https://doi.org/10.3030/769241>.
- [3] X. Sun, P. Agarwal, F. Carbonara, D. Abbott, P. Gauthier, and B. Sethi, "Numerical Investigation Into the Impact of Injector Geometrical Design Parameters on Hydrogen Micromix Combustion Characteristics," in *Volume 3: Ceramics; Coal, Biomass, Hydrogen, and Alternative Fuels*, Sep. 2020, pp. 1–11. doi: 10.1115/GT2020-16084.
- [4] ANSYS, "Reaction Design: San Diego," in *ANSYS Chemkin Theory Manual 17.0 (15151)*, 2015.
- [5] P. Agarwal, X. Sun, P. Q. Gauthier, and V. Sethi, "Injector Design Space Exploration for an Ultra-Low NOx Hydrogen Micromix Combustion System," in *Volume 3: Coal, Biomass, Hydrogen, and Alternative Fuels; Cycle Innovations; Electric Power; Industrial and Cogeneration; Organic Rankine Cycle Power Systems*, Jun. 2019, vol. 3, pp. 1–13. doi: 10.1115/GT2019-90833.
- [6] F. R. Menter, "Two-equation eddy-viscosity turbulence models for engineering applications," *AIAA J.*, vol. 32, no. 8, pp. 1598–1605, Aug. 1994, doi: 10.2514/3.12149.
- [7] Y. Liu, X. Sun, V. Sethi, D. Nalianda, Y.-G. Li, and L. Wang, "Review of modern low emissions combustion technologies for aero gas turbine engines," *Prog. Aerosp. Sci.*, vol. 94, no. October, pp. 12–45, Oct. 2017, doi: 10.1016/j.paerosci.2017.08.001.
- [8] F. Haselbach and R. Parker, "Hot end technology for advanced, low emission large civil aircraft engines," in *28th Congress of the International Council of the Aeronautical Sciences 2012, ICAS 2012*, 2012, vol. 3, pp. 2479–2490. [Online]. Available: https://www.icas.org/ICAS_ARCHIVE/ICAS2012/ABSTRACTS/306.HTM
- [9] B. Mohammad and S.-M. Jeng, "Design Procedures and a Developed Computer Code for Single Annular Combustor Preliminary Design," in *45th AIAA/ASME/SAE/ASEE Joint Propulsion Conference & Exhibit*, Aug. 2009, no. August, pp. 1–29. doi: 10.2514/6.2009-5208.
- [10] Y. Liu *et al.*, "Development and application of a preliminary design methodology for modern low emissions aero combustors," *Proc. Inst. Mech. Eng. Part A J. Power Energy*, vol. 235, no. 4, pp. 783–806, Jun. 2021, doi: 10.1177/0957650920919549.
- [11] A. H. Lefebvre and D. R. Ballal, *Gas Turbine Combustion: Alternative Fuels and Emissions*, Third Edit. CRC Press, 2010. doi: 10.1201/9781420086058.
- [12] A. T. Melconian, Jerry O. and Modak, *Combustor design. In: SAWYER, JAW. (Ed.) Sawyer's gas turbine engineering handbook design*, vol. Volume 1, no. 3rd. 1985.
- [13] D. Abbot, A. Giannotta, X. Sun, P. Gauthier, and V. Sethi, "Thermoacoustic Behaviour of a Hydrogen Micromix Aviation Gas Turbine Combustor Under Typical Flight Conditions," Jun. 2021. doi: 10.1115/GT2021-59844.

- [14] A. HORIKAWA *et al.*, “Combustor for Gas Turbine Engine,” 2015 [Online]. Available: <https://data.epo.org/publication-server/document?iDocId=5301664&iFormat=2>
- [15] M. López-Juárez, X. Sun, B. Sethi, P. Gauthier, and D. Abbott, “Characterising Hydrogen Micromix Flames: Combustion Model Calibration and Evaluation,” in *Volume 3: Ceramics; Coal, Biomass, Hydrogen, and Alternative Fuels*, Sep. 2020, pp. 1–12. doi: 10.1115/GT2020-14893.
- [16] G. Babazzi, P. Q. Gauthier, P. Agarwal, J. McClure, and V. Sethi, “NOx Emissions Predictions for a Hydrogen Micromix Combustion System,” Jun. 2019. doi: 10.1115/GT2019-90532.
- [17] G. Dahl and F. Suttrop, “Engine Control and Low NOx Combustion for Hydrogen Fuelled Aircraft Gas Turbines,” *Int. J. Hydrogen Energy*, vol. 23, no. 8, pp. 695–704, 1998.
- [18] H. H. W. Funke *et al.*, “Experimental and Numerical Study on Optimizing the Dry Low NOx Micromix Hydrogen Combustion Principle for Industrial Gas Turbine Applications,” *J. Therm. Sci. Eng. Appl.*, vol. 9, no. 2, pp. 1–10, Jun. 2017, doi: 10.1115/1.4034849.
- [19] ICAO.int, “LAQ Technology Standards.” https://www.icao.int/environmental-protection/Pages/LAQ_TechnologyStandards.aspx (accessed Apr. 23, 2021).
- [20] A. H. Lefebvre, “The Role of Fuel Preparation in Low Emissions Combustion,” in *Volume 5: Manufacturing Materials and Metallurgy; Ceramics; Structures and Dynamics; Controls, Diagnostics and Instrumentation; Education; IGTI Scholar Award*, Jun. 1995, vol. 5, no. October. doi: 10.1115/95-GT-465.
- [21] C. Marek, T. Smith, and K. Kundu, “Low Emission Hydrogen Combustors for Gas Turbines Using Lean Direct Injection,” in *41st AIAA/ASME/SAE/ASEE Joint Propulsion Conference & Exhibit*, Jul. 2005, no. July, pp. 1–27. doi: 10.2514/6.2005-3776.
- [22] D. Kroniger, M. Wirsum, A. Horikawa, K. Okada, and M. Kazari, “NOx Correlation for an Industrial 10 MW Non-Premixed Gas Turbine Combustor for High Hydrogen Fuels,” Jun. 2016. doi: 10.1115/GT2016-56189.
- [23] D. Kroniger, A. Horikawa, H. H. W. Funke, F. Pfaeffle, T. Kishimoto, and K. Okada, “Experimental and Numerical Investigation on the Effect of Pressure On Micromix Hydrogen Combustion,” in *Volume 3A: Combustion, Fuels, and Emissions*, Jun. 2021, vol. 3A-2021, no. Mmx, pp. 1–11. doi: 10.1115/GT2021-58926.
- [24] K. Tacina and C. Wey, “NASA Glenn high pressure low NOx emissions research,” *Nasa*, vol. February, no. 214974, pp. 1–6, 2008, [Online]. Available: <http://ntrs.nasa.gov/search.jsp?R=20080014197>
- [25] R. Tacina, C. P. Mao, and C. Wey, “Experimental investigation of a multiplex fuel injector module for low emission combustors,” *41st Aerosp. Sci. Meet. Exhib.*, no. January, pp. 1–16, 2003, doi: 10.2514/6.2003-827.
- [26] Z. J. He, C. T. Chang, and C. E. Follen, “NOx emissions performance and correlation equations for a multipoint LDI injector,” *53rd AIAA Aerosp. Sci. Meet.*, no. January, pp. 1–8, 2015, doi: 10.2514/6.2015-0098.
- [27] K. M. Tacina, C. Chang, Z. J. He, P. Lee, H. C. Mongia, and B. K. Dam, “A Second Generation Swirl-Venturi Lean Direct Injection Combustion Concept,” in *50th AIAA/ASME/SAE/ASEE Joint Propulsion Conference*, Jul. 2014, pp. 1–18. doi: 10.2514/6.2014-3434.

- [28] Frontline Solvers, "EXCEL SOLVER - MULTISTART METHODS FOR GLOBAL OPTIMIZATION." <https://www.solver.com/excel-solver-grg-nonlinear-solving-method-stopping-conditions>
- [29] L. S. Lasdon, R. L. Fox, and M. W. Ratner, "Nonlinear Optimization Using the Generalized Reduced Gradient Method.," *Rev Fr Autom Inf Rech Oper*, vol. 8, no. September, pp. 73–103, 1974, doi: 10.1051/ro/197408V300731.
- [30] A. P. D. Norman, D. H. Lister, M. Lecht, P. Madden, K. Park, O. Penanhoat, C. Plaisance and K. Renger, "Development of the technical basis for a new emissions parameter covering the whole aircraft operation:NEPAIR, Final Technical Report. (NEPAIR/WP4/WPR/01, and CAEP/6-IP/17 Appendix B)," 2003.
- [31] G. Ghirardo, M. P. Juniper, and M. R. Bothien, "The effect of the flame phase on thermoacoustic instabilities," *Combust. Flame*, vol. 187, pp. 165–184, Jan. 2018, doi: 10.1016/j.combustflame.2017.09.007.
- [32] EASA, "Type-Certificate Data Sheet for Trent 1000 Series Engines," 2015. [Online]. Available: <https://www.easa.europa.eu/sites/default/files/dfu/TCDS E 036 issue 15.pdf>
- [33] A. Andreini, B. Facchini, A. Giusti, and F. Turrini, "Assessment of Flame Transfer Function Formulations for the Thermoacoustic Analysis of Lean Burn Aero-engine Combustors," *Energy Procedia*, vol. 45, pp. 1422–1431, 2014, doi: 10.1016/j.egypro.2014.01.149.
- [34] U. Morgans, Prof Aimee (Department of Mechanical Engineering, Imperial College London, "OSCILOS." <https://www.oscilos.com/index.html> (accessed Feb. 27, 2023).
- [35] B. Schuermans, M. Bothien, M. Maurer, and B. Bunkute, "Combined Acoustic Damping-Cooling System for Operational Flexibility of GT26/GT24 Reheat Combustors," Jun. 2015. doi: 10.1115/GT2015-42287.
- [36] A. Horikawa *et al.*, "Combustor Development and Engine Demonstration of Micro-Mix Hydrogen Combustion Applied to M1A-17 Gas Turbine," in *Volume 3B: Combustion, Fuels, and Emissions*, Jun. 2021, pp. 1–13. doi: 10.1115/GT2021-59666.
- [37] X. Sun, D. Abbott, A. Vir Singh, P. Gauthier, and B. Sethi, "Numerical Investigation of Potential Cause of Instabilities in a Hydrogen Micromix Injector Array," Jun. 2021. doi: 10.1115/GT2021-59842.
- [38] Álvaro Fogué Robles, "Dynamics of H2-micromix arrays using CFD," Cranfield University, 2019.
- [39] D. Abbott, "The Challenges for Gas Turbine Operators of Changing Fuel Compositions and The Availability of Alternative Fuels," in *The Future of Gas Turbine Technology, 8th International Gas Turbine Conference*, 2016, p. Paper ID Number: 79 IGTC16.
- [40] C. Lahiri and F. Bake, "A review of bias flow liners for acoustic damping in gas turbine combustors," *J. Sound Vib.*, vol. 400, pp. 564–605, Jul. 2017, doi: 10.1016/j.jsv.2017.04.005.
- [41] M. R. Bothien, N. Noiray, and B. Schuermans, "A Novel Damping Device for Broadband Attenuation of Low-Frequency Combustion Pulsations in Gas Turbines," *J. Eng. Gas Turbines Power*, vol. 136, no. 4, Apr. 2014, doi: 10.1115/1.4025761.

- [42] J. Hermann, A. Orthmann, S. Hoffmann, and P. Berenbrink, "Combination of Active Instability Control and Passive Measures to Prevent Combustion Instabilities in a 260MW Heavy Duty Gas Turbine," p. 10, 2001.
- [43] "Active Instability Control." <https://www.ifta.com/en/infocenter/thermoacoustics.html> (accessed Feb. 27, 2023).
- [44] J. McClure *et al.*, "Comparison of Hydrogen Micromix Flame Transfer Functions Determined Using RANS and LES," Jun. 2019. doi: 10.1115/GT2019-90538.
- [45] P. Wolf, G. Staffelbach, L. Y. M. Gicquel, J.-D. Müller, and T. Poinsot, "Acoustic and Large Eddy Simulation studies of azimuthal modes in annular combustion chambers," *Combust. Flame*, vol. 159, no. 11, pp. 3398–3413, Nov. 2012, doi: 10.1016/j.combustflame.2012.06.016.
- [46] T. Poinsot, "Prediction and control of combustion instabilities in real engines," *Proc. Combust. Inst.*, vol. 36, no. 1, pp. 1–28, 2017, doi: 10.1016/j.proci.2016.05.007.
- [47] A. Rolt, A. Lundblad, and I. Williamson, "Roadmap for the introduction and transition to LH2 for Civil Aviation, ENABLEH2 Deliverable Report," 2022. [Online]. Available: <https://cordis.europa.eu/project/id/769241/results>

Appendix – WP3 Micromix Combustion Publications

1	P. Agarwal, X. Sun, P. Q. Gauthier, V. Sethi	Injector Design Space Exploration for an Ultra-low NO _x Hydrogen Micromix Combustion System	ASME Turbo Expo GT2019-90833	2019
2	J. McClure, D. Abbott, P. Agarwal, X. Sun, G. Babazzi, V. Sethi, P. Gauthier,	Comparison of Hydrogen Micromix Flame Transfer Functions Determined Using RANS and LES	ASME Turbo Expo GT2019-90538	2019
3	M. López-Juárez, X. Sun, V. Sethi, P. Gauthier, D. Abbott	Characterising Hydrogen Micromix Flames: Combustion Model Calibration and Evaluation	ASME Turbo Expo GT2020-14893	2020
4	X. Sun, P. Agarwal, F. Carbonara, D. Abbott, P. Gauthier, V. Sethi	Numerical Investigation into the Impact of Injector Geometrical Design Parameters on Hydrogen Micromix Combustion Characteristics	ASME Turbo Expo GT2020-16084	2020
5	M. Zghal, X. Sun, P. Q. Gauthier, V. Sethi	Comparison of Tabulated and Complex Chemistry Turbulent-Chemistry Interaction Models with High Fidelity Large Eddy Simulations on Hydrogen Flames	ASME Turbo Expo GT2020-16070	2020
6	A. Giannouloudis, X. Sun, M. Corsar, S. Booden, G. Singh, D. Abbott, D. Nalianda, V. Sethi	On the Development of an Experimental Rig for Hydrogen Micromix Combustion Testing	European Combustion Meeting	2021
7	D. Abbott, A. Giannotta, X. Sun, P. Gauthier, V. Sethi	Thermoacoustic Behaviour of a Hydrogen Micromix Aviation Gas Turbine Combustor under Typical Flight Conditions	ASME Turbo Expo GT2021-59844	2021
8	X. Sun, D. Abbott, A. V. Singh, P. Gauthier, V. Sethi	Numerical Investigation of Potential Cause of Instabilities in a Hydrogen Micromix Injector Array	ASME Turbo Expo GT2021-59842	2021
9	J. Berger	Scaling of an Aviation Hydrogen Micromix Injector Design for Industrial GT Combustion Applications	Aerotecnica Missili & Spazio, 2021, 100(3): 239-251.	2021
10	X. Sun, H. Martin, P. Gauthier, V. Sethi	Sensitivity Study on Species Diffusion Models in Turbulent Combustion of Hydrogen/Air Jet in Crossflow Structure	ASME Turbo Expo GT2022-83097	2022
11	G. Singh, M. Zghal, X. Sun, P. Gauthier, V. Sethi	Numerical Investigation into the Impact of Operating Boundary Conditions on NO _x formation in Hydrogen Micromix Combustion System	ASME Turbo Expo GT2023-103111	2023
12	N. C. W. Treleaven, S. Puggelli, R. Mercier, J. Leparoux, X. Sun, V. Sethi	High Altitude Relight Performance of Hydrogen-Air Micromix Combustion Systems	ASME Turbo Expo GT2023-103970	2023



ENABLEH2

Public Report

Final report for the single sector H2 micromix combustor segment performance and NOx emissions assessment

Authors

Xiaoxiao Sun, Vishal Sethi, Gaurav Singh, Alexandros Giannouloudis, Andrew Rolt, David Abbott, Pierre Gauthier, and Charith Wijesinghe (Cranfield University)

Nicholas Treleaven, Stefano Puggelli, Renaud Mercier, and Julien Leparoux (SAFRAN)



This project has received funding from the European Union's Horizon 2020 research and innovation programme under **grant agreement no 769241**